

AD-767 921

ARPA - NRL LASER PROGRAM

Naval Research Laboratory

Prepared for:

Advanced Research Projects Agency

June 1973

DISTRIBUTED BY:

NTIS

National Technical Information Service
U. S. DEPARTMENT OF COMMERCE
5285 Port Royal Road, Springfield Va. 22151

ARPA-NRL Laser Program

Semiannual Technical Report to Advanced Research Projects Agency 1 July-31 December 1972

*Laser Physics Branch
Optical Sciences Division*

AD 767921

June 1973



Reproduced by
NATIONAL TECHNICAL
INFORMATION SERVICE
US Department of Commerce
Springfield, VA. 22151

NAVAL RESEARCH LABORATORY
Washington, D.C.

Approved for public release: distribution unlimited.

R
69

UNCLASSIFIED

Security Classification

DOCUMENT CONTROL DATA - R & D

(Security classification of title, body of abstract and indexing annotation must be entered when the overall report is classified)

1. ORIGINATING ACTIVITY (Corporate author) Naval Research Laboratory Washington, D.C. 20390		2a. REPORT SECURITY CLASSIFICATION UNCLASSIFIED	
		2b. GROUP --	
3. REPORT TITLE ARPA-NRL LASER PROGRAM - Semiannual Technical Report to Advanced Research Projects Agency 1 July 1972 - 31 December 1972			
4. DESCRIPTIVE NOTES (Type of report and inclusive dates) Semiannual Technical Report - 1 July 1972 - 31 December 1972			
5. AUTHOR(S) (First name, middle initial, last name) Laser Physics Branch Optical Sciences Division			
6. REPORT DATE June 1973		7a. TOTAL NO. OF PAGES 4068	7b. NO. OF REFS 0
8a. CONTRACT OR GRANT NO. NRL Problems K03-08A, N01-21		9a. ORIGINATOR'S REPORT NUMBER(S) NRL Memorandum Report 2634	
b. PROJECT NO. R08-45, K03-53		9b. OTHER REPORT NO(S) (Any other numbers that may be assigned this report) N/A	
c. ARPA Order 2062 Program Code 2E20			
d. Program Element Code 62301D			
10. DISTRIBUTION STATEMENT Approved for public release; distribution unlimited.			
11. SUPPLEMENTARY NOTES N/A		12. SPONSORING MILITARY ACTIVITY Advanced Research Projects Agency Washington, D.C. 20350	
13. ABSTRACT The ARPA-NRL high energy laser program is concerned with the development of laser technology in four program areas; Chemical Lasers, Electric Discharge Lasers; High Power Glass Lasers and New Laser Techniques. The Chemical Laser Program has consisted of primarily two experiments; the development of a DF-CO ₂ supersonic transfer laser, and the study of the CO vibrational distribution from the reaction O + CS. The DF-CO ₂ device has been assembled and passivated for use with fluorine. Data on the vibrational distribution from O + CS has been obtained using a laser probe technique. Assembly of the amplifier chain of the short pulse CO ₂ laser system has continued. The nominally 1 nsec pulse that is switched out of an acousto-optically mode-locked train, has been amplified from 1 mJ to 20 mJ through the first amplifier stage. All amplifier components which will enable the system to be scaled to 30 J are expected to be in hand during the next reporting period. Under the New Laser Techniques Program a pulsed OD-CO ₂ transfer laser has been operated for the first time. The High Power Glass Laser is operating reliably and over 2000 shots have been fired during the last reporting period. This has permitted statistics to be compiled on the laser's performance and initial laser-target interaction experiments to be carried out. This report covers the progress made in the program during the first half of FY-73.			

DD FORM 1473

1 NOV 65

(PAGE 1)

UNCLASSIFIED

Security Classification

TABLE OF CONTENTS

FOREWORD.....	iii
ABSTRACT	iii
PROBLEM STATUS.....	iii
AUTHORIZATION.....	iii
CHEMICAL LASER PROGRAM.....	1
DF-CO ₂ Supersonic Transfer Chemical Laser.....	1
CO Population Distributions.....	2
SHORT PULSE CO ₂ MOLECULAR LASER.....	4
Short Pulse Oscillator.....	4
TEA Pre-Amplifiers.....	4
10 Liter e-beam Amplifier.....	5
NEW LASER TECHNIQUES.....	6
HIGH POWER GLASS LASER PROGRAM.....	7
Introduction.....	7
Control of the Self-Focusing Problem.....	7
Spatial Mode Shaping.....	8
Amplifier Train Configuration.....	8
Large Disc Amplifier. Mechanical and Electrical Design....	9
Isolation.....	12
Oscillator Stability Study.....	17
APPENDIX A - New Chemically Pumped CO ₂ and N ₂ O LASERS.....	A-1

APPENDIX B - A GLASS DISK LASER AMPLIFIER.....	B-1
APPENDIX C - DEPENDENCE OF LASER INDUCED BREAKDOWN FIELD STRENGTH ON PULSE DURATION.....	C-1
APPENDIX D - DISC LASER AMPLIFIER.....	D-1

FOREWORD

The Laser Physics Branch of the Optical Sciences Division, Naval Research Laboratory, Washington, D.C., prepared this semi-annual report on work sponsored by the Advanced Research Projects Agency, ARPA Order 2062. Co-authors of the report were J.R. Airey, O.C. Barr, L. Champagne, N. Djeu, J.P. Letellier, J.M. McMahon, S. Searles, J. Stregack, W.S. Watt and W. Whitney.

ABSTRACT

The ARPA-NRL high energy laser program is concerned with the development of laser technology in four program areas; Chemical Lasers, Electric Discharge Lasers; High Power Glass Lasers and New Laser Techniques. The Chemical Laser Program has consisted of primarily two experiments; the development of a DF-CO₂ supersonic transfer laser, and the study of the CO vibrational distribution from the reaction O + CS. The DF-CO₂ device has been assembled and passivated for use with fluorine. Data on the vibrational distribution from O + CS has been obtained using a laser probe technique.

Assembly of the amplifier chain of the short pulse CO₂ laser system has continued. The nominally 1 nsec pulse that is switched out of an acousto-optically mode-locked train, has been amplified from 1 mJ to 20 mJ through the first amplifier stage. All amplifier components which will enable the system to be scaled to 30 J are expected to be in hand during the next reporting period.

Under the New Laser Techniques Program a pulsed OD-CO₂ transfer laser has been operated for the first time.

The High Power Glass Laser is operating reliably and over 2000 shots have been fired during the last reporting period. This has permitted statistics to be compiled on the laser's performance and initial laser-target interaction experiments to be carried out.

This report covers the progress made in the program during the first half of FY-73.

PROBLEM STATUS

This is a semi-annual technical report; work is continuing.

AUTHORIZATION

NRL Problems K03-08A, N01-21, R08-45, K03-53

SEMI-ANNUAL TECHNICAL REPORT

Reporting Period
1 July 1972 - 31 December 1972

1. ARPA Order	2062
2. Program Code Number	2E20
3. Name of Contractor	Naval Research Laboratory
4. Effective Date of Contract	1 July 1972
5. Contract Expiration Date	30 June 1973
6. Amount of Contract	\$1,000,000
7. Contract Number	63201D
8. Principal Investigator	J. R. Airey
9. Telephone Number	(202) 767-3217
10. Project Scientist	W. S. Watt
11. Telephone Number	(202) 767-2028
12. Title of Work	High Power Lasers

Sponsored by
ADVANCED RESEARCH PROJECTS AGENCY
ARPA Order No. 2062

CHEMICAL LASER PROGRAM

1. DF-CO₂ Supersonic Transfer Chemical Laser

The concept of a supersonic DF-CO₂ chemical laser capable of cw operation without a vacuum pump has been discussed in detail in previous reports. Briefly it involves the addition of fluorine and deuterium at appropriate regions of combustion-driven CO₂ gasdynamic laser. These additives react to provide a source of vibrationally excited DF which then transfers energy to the CO₂ molecule. This addition of a nonequilibrium chemical-energy source shows promise as a means of upgrading the efficiency of the gasdynamic CO₂ laser.

The approach taken at NRL has been to acquire, modify and install an existing gasdynamic laser to permit DF-CO₂ supersonic chemical laser operations. These procedures along with necessary cold-flow tests and preliminary combustion-chamber firings were completed during the last reporting period.

During this last six months we have been concerned with the establishment of proper flow conditions in preparation for the introduction of fluorine and deuterium into the gas flow. In particular these efforts were concentrated toward assuring that complete conversion of CO to CO₂ is accomplished in the combustion chamber and testing the modified diffuser system. Completion of these tasks was followed by complete disassembly, cleaning and reassembly of the apparatus. This preparation was required before fluorine could be safely introduced into the apparatus. Passivation of the apparatus was the final task completed during the present reporting period.

Complete oxidation of the CO to CO₂ is required to prevent the formation of COF₂ by the reaction of CO with F₂. In addition to depleting the fluorine concentration, the formation of COF₂ has been recognized as a potential loss mechanism in the DF-CO₂ laser system as a result of its absorption near 10 μ and as a deactivator of the CO₂ upper laser level. Measurements of the composition of the combusted gas have been made for an extensive series of test firings with a wide range of initial gas flow-rates. In all cases where there was satisfactory combustion initiation and an excess of oxygen concentration the amount of carbon monoxide remaining was always below 0.5% of its initial value. Conversion of this amount of CO to COF₂ is estimated to have a negligible effect on the DF-CO₂ laser performance.

One of the key technical aspects of the present program is to achieve full atmospheric pressure recovery. With the mode of operation of the present device, the diffuser initially experiences a supersonic flow whose Mach number is $M \approx 4.5$. Upon initiation of the D_2/F_2 chemistry there is an increase in temperature and pressure of the gas entering the diffuser which is accompanied by a reduction in Mach number. Thus the diffuser is required to operate reliably over a wide range of gasdynamic conditions. In particular, it is important that the chemical energy addition does not dislodge the shock wave from the diffuser as this would result in a shock wave sitting in the nozzles. The resulting high-pressure, high temperature gas would probably be in a non-inverted state and would not lase.

In an extensive series of tests, the diffuser performance has been examined as a function of combustor temperature, pressure and gas composition. Briefly, the diffuser requires a combustor pressure above ~ 230 psi to start and atmospheric pressure recovery is maintained as long as the steady-flow pressure is greater than ~ 200 psi. For the maximum CO delivery rate a gas mixture which contained only helium as a diluent was found to attain insufficient combustor pressure to reliably start the diffuser. Substitution of a portion of the helium with nitrogen serves to raise the combustor pressure at the expense of combustor temperature with a corresponding improvement in the diffuser performance. By replacing approximately 15% of the helium with nitrogen a series of conditions have been established where the diffuser performance could not be faulted. Experiments will shortly be initiated to investigate the effect of chemical energy addition on these conditions. Meanwhile modifications to the combustion chamber are planned to allow a greater CO delivery rate at which higher combustion pressures will be attained.

2. CO Population Distributions

Preliminary results have been obtained on the initial vibrational distribution of CO from the reaction $O + CS$. While the data are quite reproducible, further instrumentation will be needed to prove that the distribution is unrelaxed.

The experiment is set up as follows. Discharged oxygen containing about 25% O atoms is brought to react with CS_2 in a tube fitted with Brewster's windows. The tube is connected to a high-capacity diffusion pump, so that the residence time of an average product CO molecule in the tube is about one millisecond. The apparatus is situated inside a cw CO laser cavity. The oscillation range of the single-mode frequency-tuning curve of the laser is measured with and without CS_2 injection into the reactor. The optical gain or loss introduced by the reaction $O + CS$ is then calculated. This is done for about half a dozen transitions in each band so that the inversion ratio between

the two connected vibrational levels can be determined.

Experiments have thus far been carried out for CO product pressures of 10 and 20 millitorr. Inversion ratios were obtained for the $v = 15 \leftrightarrow v = 14$ down to the $v = 4 \leftrightarrow v = 3$ bands. In both cases, except for the highest band, which showed an inversion ratio of about 0.4, all N_v/N_{v-1} were measured to be between 0.8 and 0.9. At the pressures used, each CO molecule could collide with another CO in a neighboring vibrational level a number of times in the one millisecond residence time. Hence, it is possible that the distributions measured thus far have undergone some V-V relaxation.

At present, a new reactor apparatus is being built to afford a residence time sufficiently short to insure no V-V relaxation of the CO product. Also, a different probe laser is being constructed which hopefully will operate down to the $v = 2 \leftrightarrow v = 1$ band.

SHORT PULSE CO₂ MOLECULAR LASER

The system design for the short pulse high energy laser has been reworked to include five NRL-built solid Rogowski electrode amplifiers, two Lumonics Series 600 amplifiers, and an electron beam excited amplifier. The first Rogowski electrode amplifier has a discharge volume of 2 x 2 x 100 cm. The next four amplifiers have discharge volumes of 3 x 3 x 50 cm each. A two power beam expander scales the beam up to the Lumonics amplifiers which have discharge volumes of 9 x 9 x 50 cm each. The electron beam excited amplifier has a discharge volume of 10 x 10 x 100 cm and will be operable up to 2.5 atmospheres pressure. The major change in the system is the elimination of the segmented cathode amplifier which utilizes surface preionization created by corona discharges between metal blades and glass rods. This amplifier required too much maintenance in the form of replacement of broken glass rods. We found that the solid electrode UV initiated amplifiers achieved higher peak gains, better pulse to pulse reliability, and were much more durable. Additional stages of amplification were added because of preliminary measurements which indicated that the saturation energy flux for short pulses may be a factor of three lower than calculations predict.

1. Short Pulse Oscillator

An atmospheric pressure CO₂ oscillator has been acousto-optically mode-locked with a Brewster-angle germanium crystal. A single nanosecond pulse has been switched out of the train of mode-locked pulses with a GaAs Pockel's cell activated by a laser-triggered spark-gap. The switched-out pulse energy has been increased from 1 mJ to 20 mJ through one stage of amplification. Recent experiments have focused on increasing the reliability of this system.

2. TEA Pre-Amplifiers

Two types of volume TEA discharges were investigated as short pulse preamplifier elements. One utilizes two solid Rogowski electrodes with volume preionization created by UV emission from an auxiliary discharge. The other utilizes a segmented cathode with surface preionization created by corona discharges between metal blades and glass rods. The problems uncovered with the latter design caused it to be dropped from the system.

The solid electrode design is very promising. Repeatable glow discharges have been obtained in a 50% He, 25% CO₂, 25% N₂ mixture

with an energy input of 250 joules per liter in the 2 x 2 x 100 cm device. Energy inputs to the 3 x 3 x 50 cm amplifiers have been 350 joules per liter. The measured small signal gain coefficient is in excess of $3\% \text{ cm}^{-1}$. The pulse to pulse reproducibility is better than 90%.

We have tested resistor pin and wire type auxiliary preionizing discharges. The resistor pin discharges provided more reliable operation at low CO_2 concentrations, but the wire type discharges were superior at high CO_2 concentrations. The addition of small percentages of hydrogen allowed slightly higher energy inputs without arcing, but the benefit was so slight that we discontinued its use.

Small signal gain measurements of the 3 x 3 x 50 cm amplifiers indicated that self-oscillation was occurring between the highly polished electrodes. We found that a light sandblasting of the electrode surface reduced specular reflectance from $> 95\%$ to $< 10\%$. The self oscillation was suppressed without the discharge properties being changed.

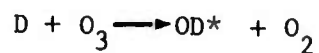
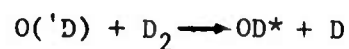
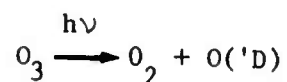
The delivery of the Lumonics amplifiers has been delayed to March because they are experimenting with a new preionization arrangement which they feel will be superior.

3. 10 Liter e-beam Amplifier

A design review was held in December at Maxwell Laboratories between Maxwell and NRL representatives. The design appeared to be satisfactory with minor modifications being made. The device is scheduled for testing at Maxwell in May and delivery in mid-June.

NEW LASER TECHNIQUES

The effort to find new laser systems during this reporting period has produced a new chemical CO₂ laser, the OD-CO₂ system. The attractive feature of this laser is that the reaction products are completely harmless, as compared to the effluent of the DF-CO₂ system. Laser pulses were obtained from the OD-CO₂ system when mixtures of D₂, O₃, CO₂, and He were flash photolyzed. The pumping mechanism is believed to be the following:



Peak powers in the neighborhood of 1 kW have been obtained from this laser. The results of this work will appear in Applied Physics Letters shortly, and a preprint of this paper is included in the Appendix.

Another project under this New Laser Techniques heading, the double pulse excitation experiment, has made great progress in the last six months. The construction of the electronics has now been completed. The DC circuitry is capable of generating a 1 μsec pulse with a rise time of 0.1 μsec, at 8 kV and 25 A. This is followed by a similar RF pulse, with the separation between the two pulses being adjustable to any desired time. It is anticipated that experimentation with this novel excitation scheme will begin shortly, after the completion of the other hardware parts.

HIGH POWER GLASS LASER PROGRAM

Introduction

At the close of the laser reporting period solutions were thought to be in hand for most problems afflicting the NRL system when used for subnanosecond operation. The system was moving into a stage of routine operation for target shooting for DNA and AEC/OST funded programs. Basic techniques for controlling spatial and temporal beam characteristics to prevent self focusing had been worked out. Realignment of the system incorporating these techniques began in late July 1972 with target shooting commencing on 21 August 1972.

The over 2000 shots on the system since then have allowed study of technical and economic factors involved in operation of a large glass laser system. The large number of shots have allowed reasonable statistics to be gathered not only of the target behavior but also of the laser's behavior. Operation of the system over this reporting period attests to the utility of the techniques developed. This has allowed us to turn our attention to questions of reliability, maintainability, long term stability and repeatability, and target backscatter isolation.

Control of the Self-Focusing Problem

At the close of the first reporting period we reported on several optical modifications to the French system to make it more compatible with short pulse operation. Our self-focusing measurements indicated that the nonlinear index of refraction was a constant for short pulses ($20 \text{ psec} < \tau < 1 \text{ nsec}$). The measured values for ED-2, LG-56 and MG-915 laser^pglasses indicated that $n_2 \sim 7 \times 10^{-4} \text{ esu}$ ($\sim 10^{-15} \text{ cm}^2/\text{watt}$).

There are several immediate systems consequences of these observations:

- time bandwidth limited pulses will have higher damage thresholds than pulses with temporal structure since self focusing can follow picosecond temporal structure;
- n_2 is large enough for the laser glasses that some dynamic wavefront distortion will be present in terawatt level systems; and
- n_2 is large enough that spectral broadening due to self phase modulation has to be considered.

The implementation of these considerations consisted of

- oscillator modifications to ensure time-bandwidth limited operation. This was done by making the oscillator front mirror be the bandwidth selecting etalon;
- minimization of the glass path length in the system since both self phase modulation and wavefront distortion will vary as

$$\propto n_2 \int_0^L P(l) dl;$$

- staging the output level of the amplifiers as the square of the area to make gross self focusing equally unlikely through the system and also to minimize self phase modulation and wavefront distortion.

During the present reporting period we have carried this work forward into the area of improved spatial beam quality and have concentrated on what practical levels of operation can be achieved routinely.

Spatial Mode Shaping

While a TEM₀₀ oscillator mode is certainly optimal in the oscillator it is not the most desirable mode for propagation through amplifiers for the basic reason that the intensity does not approach zero radially for many beam diameters. This causes Fresnel diffraction from apertures and the Fresnel rings will self focus. This led us to try various apodization techniques to suppress the wings of the Gaussian with minimum penalty in spatial ripple due to the apodization. The technique we have found most successful to date is a two step truncation procedure using hard apertures. This approach consists of truncating the TEM₀₀ mode after the oscillator and then truncating at the first dark ring of the Airy disc ≈ 8 meters away. Truncating at the e^{-4} point induces spatial ripple of $< 1\%$ in the near field of the second aperture.

Amplifier Train Configuration

Following the general "less is better" philosophy, it was possible to eliminate the 16 mm rod amplifier by driving the 23 mm and 32 mm amplifiers harder. Improved flashlamps obtained from ILC as well as the higher gain of Owens Illinois glass have allowed us to do so without any penalty in reliability.

The result of these fixes has been to allow routine operation of the system through the 45 mm amplifier with no short term degradation. In

~ 2000 shots on the AEC and DNA programs the only long term degradation noted is that the 45 mm amplifier rod has to be replaced every 500 - 600 shots due to accumulated damage although on a single shot no damage is observable. The causes of the degradation over many shots appears to be basically alignment errors in routine operation compounding the fact that the margin for error is very slight for this rod. In this amplifier the peak power density at the input is $\approx 3 \times 10^9$ w/cm² and $\sim 2 \times 10^{10}$ w/cm² at the output.

The 64 mm rod amplifier has proven to be not useful for routine operation in that damage will occur in a few shots and degradation of the useful output level will occur in ~ 50 shots as noted in the last report. There are several factors which compound the problem:

- the power density is very high through the rod. 10^{10} w/cm² at the input and 4×10^{10} w/cm² at the output;
- any alignment error giving rise to 2% spatial modulation on a millimeter diameter scale will cause self focusing in the rod due to the long length;
- high optical quality rods of this size (2000 cm³) are essentially unobtainable at this time.

Disc amplifiers appear to have a much higher tolerance for structure on the beam in that we have run in excess of 2×10^{10} w/cm² with no evidence of self focusing damage and the University of Rochester has reported even higher levels. This seems plausible in that very high power densities are required to focus in a single disc; additionally, focusing through a series of discs should not lead to the large scale beam steering effects observed in rods since most of the path length is in air with a small value of n_2 ($\approx 7 \times 10^{-15}$ esu) rather than in glass.

The solution we are pursuing to this problem is to replace the 64 mm rod with a 44 mm disc amplifier using the same pump cavity for the small disc amplifier that was used for the 64 mm rod. In this helically pumped disc amplifier we expect a small signal gain of $\approx 7 - 8$ db and in the system expect it to amplify the output of the 45 mm rod to $\sim 60 - 70$ joules. This will then be fed to three new 65 mm disc modules to amplify the pulse to ≈ 500 J.

Large Disc Amplifier. Mechanical and Electrical Design.

The 65 mm aperture amplifier has been used to study the physics of energy storage and extraction and in that sense has served as a prototype for the 15 cm aperture amplifier (Appendix A). In a

similar fashion, it seemed wise to prototype the mechanical and electrical designs on the smaller amplifier. Problems could then be identified and solved before they were scaled up to an overwhelming level.

Use of the present ARPA/NRL disc amplifier during the past year had revealed a number of inconveniences which interfere with its use on a day-in-day-out basis. Mechanical and electrical redesign would both serve as a prototype for the proposed 15 cm amplifier and significantly reduce the number of man hours of labor required to sustain normal operations at 100 + shots on target per week when operating.

Specific problems that have been identified for action are

- rapid degradation of transmission due to accumulation of dirt on discs;
- fixed orientation (vertical polarization) which places constraints on the system isolation design;
- high voltage arc-overs on cables from the capacitor bank.

Two fixes have been incorporated in the present disc amplifier to help with disc cleanliness. The disc holders had been gold plated aluminum. However, in order to put on the gold, the aluminum is first plated with zinc. Sufficient flashlamp light is absorbed by the gold to boil the zinc, throwing gold fragments on the glass discs. The gold and zinc have been removed from the disc holders and the aluminum then was chemically and mechanically polished. This has proven to be quite satisfactory. The reflectors remain gold plated brass. Filters have been placed in the nitrogen lines which are used to purge the head during a shot.

ILC Technology Inc. of Sunnyvale, California, the manufacturer of the flashlamps, has been contracted with to design, fabricate, and deliver a prototype module. This will be six discs (compared to the present 11) to reduce weight and balance problems on the head mounts. One constraint placed on this design is that the discs are to be sealed in an air tight, nitrogen purged chamber. They are separated from the flashlamps by Pyrex shields, allowing servicing the lamps without exposing the discs to the atmosphere. The present structure is, of course, nitrogen purged during a shot to prevent acoustic shock waves due to oxygen absorption of ultraviolet lamp radiation, but the structure is completely open to the atmosphere between shots.

Experience with sealed stacked plate polarizers indicate that limiting exposure to the atmosphere indeed preserves glass cleanliness. Additionally, a disc amplifier retrofit for the 64 mm French amplifier

has been developed, which is completely sealed and purged with N_2 . With it a quantitative answer will be obtained for how frequently such an amplifier must be disassembled for cleaning.

The frequent lamp failures experienced have been mainly restricted to seal failures. New mounts for the lamp ends have been devised and installed on the ground end of the lamps in the present head. High voltage limitations prevented installation of the new mounts of both ends in the present head. Initial results indicate a significant reduction in seal failures.

ILC was awarded a contract to work on this problem. The work has been completed and a copy of their report is included (Appendix D). The basic results were that they modified the NRL lamp mount to eliminate the high voltage arcing problem. This allowed mounting the lamps with currents reversed in adjacent lamps, reducing magnetic fields in the head by a factor of 20. They conducted life tests to failure for lamps with large length to diameter ratios. These tests confirmed that the basic life formulas derived from small lamps are valid for these large lamps⁽¹⁾. As a final test ILC built a test jig representing 1/2 of the new disc amplifier cavity and ran 500 shots at maximum energy on the flashlamps. All these results are being incorporated in the new design⁽²⁾.

The ILC design is proceeding in such a manner that the entire head can be rotated $\pm 180^\circ$ to accommodate any polarization dictated by the system isolation requirements. The stacked plate polarizers and the disc amplifier retrofit for the French 64 mm head have been designed for 360° rotation for similar reasons.

1. The lamp is given a single shot explosion rating

$$E_{ex} \text{ (joules)} = 20,000 \ell dt^{\frac{1}{2}}$$

where ℓ (length) and d (diameter) are in cm and t is the characteristic time constant \sqrt{LC} of the single mesh drive circuit. t is thus $\approx 1/3$ of the full width current pulse in seconds. The lifetime is then approximately $(E_{ex}/E)^{8.5}$ where E is the actual lamp loading (joules per shot). These were determined experimentally for lamps of 4 mm bore and 2 inch arc length.

2. The first ILC effort relating to lamp life was funded to a level of \$24 K. The second phase, involving delivery of an actual amplifier module, is a \$31 K effort. It is anticipated that three additional modules will be procured for \$12 - 15 K each.

The high voltage arcing of the drive cables has been analyzed. Basically, the present load cables (Amphenol 21412) were selected because of their small size. This leads to small radii of curvature of the insulation on the center conductor and allows arcs to form on the outside of the insulation and travel (track) along it to ground. Return to RG-8/RF-213 cable seemed the simplest solution. The test modules delivered to ILC for their test program used RG-8 cables. No problems were encountered and thus the present head is being retrofitted to RG-8 as time is available. Temporary anti-ringup fixes have been put on the unconverted capacitor bank modules until all are converted to RG-8 cables.

Emphasis should be placed on the current utilization of the original amplifier. Present operations follow the pattern of disassembly and cleaning of the discs every Monday. The amplifier is reassembled and operations started by Tuesday noon. Twenty to thirty shots per day can be achieved from then thru Friday evening. Routine operation (limited by isolation from target back scatter) at 60 joules on targets of CD_2 and high Z metals with peaks of 100 joules have been achieved. It is anticipated that the routine will move to over 100-joules and with installation of the 64 mm head modified with discs, operation to 200 J on target will be reached in May 1973.

Isolation

In order to use the laser system for irradiating targets for the DNA funded x-ray generation program and the AEC/OST funded laser induced fusion program, it was necessary to isolate the laser from the back-reflected light from the target. Although this has been done on DNA and AEC funding, a short description is included here for informational purposes.

A simple statement of the problem is that lasers are bi-directional amplifiers. A one millijoule pulse from the oscillator is amplified (outgoing) to 100 J for a gain of 50 db. Small signal gains of 60 to 70 db are typical. A 1% reflection back into the laser (1 J) is amplified backwards until some component simply vanishes.

Two factors tend to magnify the scale of the disaster. Subnanosecond pulses are shorter than the lower state lifetime of Nd glass. Thus in even heavily saturated amplifiers the outgoing pulse can extract only 50% of the stored energy (for single pass amplifiers, 75% for double pass, etc). The target reflection, some 200 nsec later (in the NRL case) has essentially the same gain as the outgoing pulse.

The outgoing pulse is diverging through the amplifiers to maintain a peak power density of $\leq 10^{10}$ w/cm². The reflected pulse is converging as it is amplified. Further, it is not safe to assume that a point

in the laser can tolerate the same energy in both directions. The outgoing pulse is carefully shaped spatially and temporally to minimize the chances of self focusing. The back reflected pulse may not have as clean a profile. In the NRL system, components are derated by a factor of 2 to 10 for the back reflected pulse, depending on their tendency to suffer from self focusing of the beam.

Isolation considerations can be divided into two interrelated areas: system configuration and component design. System design takes into consideration desired safety levels, expected target backscatter characteristics, amplifier gains and optical losses within the constraints set by physically realizable isolation component specifications and practical alignment accuracies. The components must then be designed to meet and maintain the performance levels demanded by the system and must be capable of being aligned by simple, straightforward means.

The basic objective set for the system design was to protect the system from a reflection representing 100% of the outgoing energy (assumed to be 500 J for the final configuration of the present system) whose polarization could be rotated to any arbitrary angle with respect to the polarization of the outgoing beam. The case of a perfectly aligned system was first analyzed since the worst case polarizations are always parallel to and perpendicular to that of the outgoing beam. Then an analysis was made of the degradation caused by reasonable misalignments of individual components and then groups of components. For these cases all possible polarizations must be considered. Finally, system configurations are iterated to minimize component count and alignment accuracy requirements.

It is in fact reasonable to assume a system requirement of withstanding 100% of 500 J back reflection. It is possible to achieve this level of protection with real components although the safety margin does not encourage routine operation in this regime⁽¹⁾. At expected routine levels of 250 - 350 J, the safety margins are very comfortable and with reflections nearer 1% rather than 100%, no damage should be seen. This extra margin of safety will allow demonstration of one or two 15 cm amplifiers on the system after the final isolator without requiring additional, large aperture, isolators. Components have been designed for this final system configuration and those in hand have been used for intermediate level operations. One such system configuration that has been used at NRL is shown in Figures 1 and 2. It is typical of the way the various components can be arranged and its performance has been verified. Specifications were set at 100 J on target and a safe back reflection of 10 J of arbitrary polarization.

1. French AEC experimenters have reported 40% reflections back into their high power glass laser.

The discussion now switches to a component by component discussion starting from the output end. Due to lack of an adequate piece of Faraday rotator glass to withstand the energy density at the disc amplifier output this amplifier was located after the last isolation element. This set the 10 J reflection limit for this configuration. Table 1 shows stage by stage levels.

The output polarizer (No. 2) consisted of 6 plates of BK-7 glass. Plates are wedged 1° and fanned for an angle of incidence of 58° to 59° per surface, slightly greater than Brewster's angle. Transmission of 95% for the transmitted polarization and 10% for the rejected polarization were achieved. Additional plates could improve rejection to 26 db with transmission of $> 90\%$. Better rejection ratios are difficult to achieve due to surface scatter.

The 65 mm aperture amplifier, operating at 35% pump energy, has a small signal gain of 5 and a cross polarized transmission of 20%.

The Faraday rotators consist of a 2 cm thick 8 cm aperture piece of Owens Illinois EY-1 glass in a 34 kilogauss magnetic field. The polarization is rotated 45° outgoing and an additional 45° upon reflection. Rotator 2 operates on the reflected light polarized parallel to the outgoing beam and rotator 1 kills the perpendicularly polarized components. Magnetic field uniformities of 1% have been measured, adequate for 40 db rejection between perfect polarizers. Rejections of -30 db for rotator 1 and -34 db for rotator 2 have been measured when double internal reflections within the glass are spatially filtered out. These limits are set by inclusions in presently available samples of EY-1⁽¹⁾.

Polarizer No. 1 is similar to No. 2 except it has 12 plates and a rejection of 20 db (1%) with a transmission of 94%.

1. Owens Illinois delivered the present two pieces under a \$10 K best effort contract. They have received \$50 K from AEC labs to further improve the glass optical quality.

TABLE I
APPROXIMATE REFLECTED ENERGY LEVELS IN SYSTEM

<u>COMPONENT</u>	<u>POLARIZATION</u>		<u>OUTGOING LEVEL</u>
	<u>11</u>	<u>1</u>	
Output face of polarizer 2	10 J	10 J	120 J
Input face of polarizer 2	10	1	
Input face disc amplifier	50	.2	
Input face polarizer 1	.5	.2	30
Input face 64 mm rod	1	.4	
Output face 45 mm rod	.01	.4	15
Output face rotator 1	.001	3.2	
Output face 32 mm rod	.001	.004	4
Input face 32 mm rod	.02	.06	
Output face Pockel's cell	.02	.001	
Output face 23 mm rod	.00002	.001	.2
Mirror	.0002	.01	.07

The rod amplifiers using the French cavities have the following properties.

<u>APERTURE</u>	<u>GLASS</u>	<u>SMALL SIGNAL GAIN</u>	<u>TYPICAL OUTPUT ENERGY</u>
64mm	LG-56	2X (3 db)	30 J
45mm	ED-2	6X (8 db)	15 J
32mm	ED-2	20X (13 db)	4 J
23mm	ED-2	10X (10 db)	.25 J

In all cases the birefringence is assumed to be 1% based on our worst case measurements. When this system was operating the flashlamp currents in the 64 mm head were alternated for zero Faraday rotation. The rotation in the 45 and 32 mm heads was on the order of a few degrees, causing unnecessary losses for the outgoing beam. The lamps in the 45 mm head have since been alternated and the 32 and 23 mm heads will soon be similarly modified.

Thin film polarizing coatings on BK-7 glass substrates have been obtained from Laser Energy Inc. of Rochester, N.Y. Their properties are rejection ≈ 20 db and transmission $> 95\%$ for an angle of incidence of 60° . The polarizer located after the 45 mm amplifier, operating at a beam energy density of 2 J/cm^2 ($\approx 1 \text{ J/cm}^2$ on the coating) damaged after 50 - 100 shots at 0.9 ns pulsewidth. The plates at other locations have survived beam energy densities of 1 J/cm^2 and continue to show no sign of damage.

Pockel's cell No. 2, of 27 mm aperture, is pulsed to 90° rotation for the outgoing pulse and rests at 0° rotation for the reflection. Residual birefringence in the KD*P crystal limits reject by crossed polarizers to about 32 db. A much lower level of performance is demanded in this particular system configuration. Safe operation at 1 J/cm² is assumed and a transmission of 90% is reasonable.

Calcite and KD*P glan prisms have been used here. Extinctions of -50 db are possible between crossed high quality prisms. The penalty is that transmission is reduced to about 50% per prism. By misaligning the prisms for an extinction of about -30 db (comparable to the limits set by the Pockel's cell birefringence), transmissions of 87% are achieved. The LEI polarizers appear to be a preferable way to go, especially at large apertures where it is desirable to minimize losses for the outgoing pulse. Safe subnanosecond levels of 1 J/cm² are assumed although no single shot damage has been observed at 3 J/cm².

The turning mirrors live at 1 J/cm² or 0.1 J total energy. Any level safe on them is safe for the YAG amplifiers and oscillator so the isolation analysis ends at the turning mirrors.

The final system consideration is a failure analysis. The isolation depends upon both Pockel's cells and Faraday rotators. Our practice with Pockel's cells is to apply an electric field (10 - 12 kV total, duration 5 - 20 ns) to the crystal when the outgoing pulse is expected to pass through and remove the field afterwards. Improper timing will kill the output pulse and incorrect voltages will cause excessive losses. When the reflection returns to the Pockel's cell, it is at zero volts, a level that can be achieved with great precision and high field uniformity across the aperture. This maximizes the extinction ratio of the Pockel's cell. The electrical pulse is generated by a pulse forming transmission line charged by a low current power supply, thus a second pulse is not possible as the network can not recharge in the 200 nsec period. Failure of the Pockel's cell kills the outgoing pulse but always leaves the system in its maximum protection state for any back reflection.

The same is not true for the Faraday rotators. They are designed for 45° rotation per pass, thus the polarizers located before and after each rotator are only 45° rather than 90° apart. If a rotator fails, the outgoing beam suffers only a 3 db loss, rather than the 20-30 db with a similar failure in a Pockel's cell. The back reflection protection of -20 to -26 db anticipated also becomes -3 db if the rotator magnetic field is gone. Thus the total protection anticipated for a failed Faraday rotator is 6 db (3 db outgoing and 3 db reflection) rather than 26 db. The approach taken at NRL is to use a long, flat topped current pulse (top flat $\pm 1\%$ for 90 - 100 μ sec). The current is carefully measured after it reaches its peak. If it is out of tolerance,

no voltage pulse is applied to Pockel's cell No. 2, killing the outgoing pulse there and averting disaster.

Oscillator Stability Study

In the course of setting up a second mode locked Nd:YAG system for prepulse and pulse shaping studies on the DNA contract, we took the opportunity to perform some studies on the stability of the mode-locked YAG system developed for ARPA in preceeding years. A photodiode-integrator-pulse height analyzer combination was used to determine the distribution of pulses in energy. The inherent resolution of the system was determined to be better than $\pm 1\%$. In typical situations 5000 to 50,000 pulses were run with an oscillator set up identically to the fashion in which the master oscillator on the French laser. The distribution was found to have a width corresponding to $\pm 5\%$ reproducibility.

A comparison was run between a poorly regulated power supply and a .01% voltage regulated KEPCO power supply (which is used in the laser master oscillator). The distribution for the poorly regulated supply had a width of $\pm 7.5\%$ while the well regulated supply a width of $\pm 5\%$. A sinmer supply was tried with both power supplies to see if it would stabilize the arc. It did not appear to improve the situation in either case.

Our first guess as to the cause of this lack of reproducibility was that the arc in the flashlamp did not fill the bore and from shot to shot would not behave in a reproducible fashion. A 2 mm bore flashlamp was then substituted for the 4 mm bore flashlamp. This produced a marked improvement with both power supplies. The distribution widths were $\pm 5\%$ and $\pm 3\%$ respectively. Various checks for thermal instabilities in the rod revealed that these did not seem operative and that the sleeved rods had no apparent thermal transients.

It was found that the absorption coefficient of the mode locking dye changed by $\approx -1\%/^{\circ}\text{C}$, which could lead to long term thermal drifts in the output. The dye was therefore stabilized to nominal room temperature ($24^{\circ}\text{C} \pm .1^{\circ}\text{C}$).

It was also found (not surprisingly) that bandwidth limiting etalons had to be stabilized to $\pm 1^{\circ}\text{C}$ to avoid thermal drifts in the output.

At present the limit appears to be the switching reproducibility of the saturable absorbers and attempts are being made to improve this via filtration to remove particles in suspension and surge chambers to minimize vibration and pressure gradients.

The reproducibility level achieved to date appears adequate for system operation. It also appears that while $\pm 1\%$ operation may be hoped for, $\pm 0.1\%$ operation will be difficult to achieve.

This oscillator was run for some fundamental studies on avalanche breakdown in solids in cooperation with Harvard University and Raytheon (Appendix C).

APPENDIX A

NEW CHEMICALLY PUMPED CO₂ AND N₂O LASERS*

S.K. Searles and J.R. Airey

Optical Sciences Division
Naval Research Laboratory
Washington, D.C. 20375

*This work was supported by Naval Ordnance Systems Command PMO 405 and ARPA Order 2062.

ABSTRACT

Laser oscillation, based on the transfer of vibrational energy from OD(OH) to CO₂ and OD to N₂O, was observed during the flash photolysis of mixtures containing ozone.

Pulsed CO₂ lasers^(1,2) have been pumped by energy transfer from vibrationally excited HCl and DF(HF) produced in chemical reactions. Recently an efficient reaction mechanism was proposed for an OH-CO₂ transfer laser.⁽³⁾ We wish to report detection of optical gain and subsequent laser emission from the flash photolysis of O₃ - D₂(H₂) - CO₂ and O₃ - D₂ - N₂O mixtures.

The experimental apparatus consisted of a 3m optical cavity formed by a 4m maximum reflectivity dielectric mirror and a 4m gold coated mirror with either a 1 or 2 mm hole for output coupling. Along the optical axis within the cavity there were two units. One unit was a 1.5m conventional electrically driven gain tube. The other was a flash photolysis unit. This contained six lamps which pumped 75 cm of the 110 cm long 2.5 cm diameter fused silica tube which was fitted with Brewster angle windows. The photolysis pulse had a 12 μ sec FWHM. Typically the flash energy was 1500 J. Laser output was detected by a gold doped germanium detector after passing through a germanium filter. The detector output was displayed on an oscilloscope which could be triggered by the initiation of the photo-flash.

The experimental work commenced by probing CO₂ mixtures in the photolysis unit. The operation of the gain tube was adjusted so that laser oscillation occurred near threshold. Specifically a gain of 0.2% greater than the cavity loss was found to give a reliable operation. The effect of this arrangement is to create a nearly zero loss optical cavity at one line in the CO₂ band for the intracavity flash photolysis system. Thus a small change in gain during a flash could result in a substantial amplification of the laser output signal. The composition of the flashed gases was varied to maximize the peak laser power enhancement.

The first probe experiments were with O₃ - CO₂ mixtures. These mixtures were not expected to give amplification but were intended as a check on the overall operation. However, laser power enhancement occurred. A peak factor of 80 was obtained from a flashed mixture 0.9 torr O₃ and 3.7 CO₂. The pulse width at half maximum (amplification factor of 40 for this experiment) was 14 μ sec. In further trials, independent laser oscillation (that is, with the probe laser switched off) was not observed.

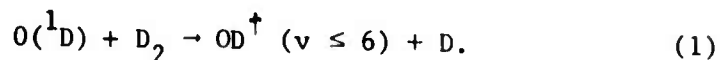
After a number of probe experiments involving different partial pressures of O_3 , CO_2 and D_2 were carried out, the electrical discharge was turned off. The next experiment gave independent laser action. With 0.85 torr O_3 , the peak power was found to be independent of the total pressure over the range 30 - 180 torr for an equimolar $CO_2 - D_2$ situation. The peak power was 250 W and the maximum energy was ~ 0.7 mJ as determined by a calibration of the detector against an Eppley thermopile. An oscillograph of the laser pulse is shown in Fig. 1. Use of a 2 mm coupling hole instead of the 1 mm coupling hole gave approximately the same laser power. Reflashing a gaseous mixture yielded about 10% of the power obtained from the original mixture. Two experiments were carried out with added CO. 20 torr of CO quenched laser action while 5 torr only slightly reduced the laser signal. Substitution of H_2 for D_2 gave a 60% reduction in power. A spectrographic determination of the laser transitions showed the P(12) - P(24) lines to be present.

Replacement of the CO_2 by N_2O gave laser emission on the P(14) to P(24) lines. Peak power was 50 W in the $O_3 - D_2 - N_2O$ mixtures while $O_3 - H_2 - CO_2$ mixtures did not lase.

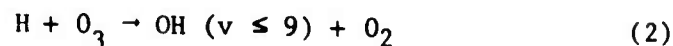
The reaction chemistry leading to the new lasers reported here is sufficiently complex and unknown that a probe device was needed to find a mixture which would give independent laser action. However some of the mechanism is known with certainty. The primary act in the flash is the production of $O(^1D)$ and $O_2(^1\Delta_g)$ from O_3 .⁽⁴⁾ The role of $O_2(^1\Delta_g)$ is ignored because of its low reactivity with the reagents.⁽⁵⁾ In contrast $O(^1D)$ is highly reactive and is consumed either by energy transfer or reaction at nearly every collision with O_3 , CO_2 , or D_2 .^(4,6)

In mixtures without D_2 the inversion in CO_2 is most probably caused directly by energy transfer from $O(^1D)$ to the ν_3 mode of CO_2 .

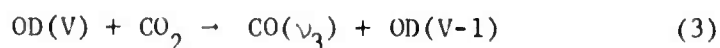
Addition of D_2 to the mixture provides an additional path for removal of $O(^1D)$. In a 1:1 mix of D_2 and CO_2 with these gases in excess of O_3 , approximately half of the $O(^1D)$ reacts with D_2 according to



A subsequent additional source of OD^{\dagger} is the reaction of D with O_3 . Charters et al.⁽⁷⁾ have shown that for



the major fraction of the reaction exothermicity appears as vibration in OH. Also the reaction rate is fast due to a high rate constant⁽⁸⁾ and high ozone concentration. The fact that laser emission occurs upon reflashing a mixture demonstrates that not all the ozone is decomposed in a single flash. Therefore, the O₃ concentration during the first flash is expected to be sufficiently great that reaction (2) will make a useful contribution to the total OD[†] production. Further study is necessary to establish the relative importance of the two sources of OD[†]. Reaction (3) then populates CO₂(v₃). The rate of energy transfer



has not been measured though it may be expected, by analogy with the measured DF[†]-CO₂ rates⁽⁹⁾, to be fast. The high concentrations of D₂ and CO₂ that are required for optimum laser power indicates deleterious side reactions involving either O₃ or reaction intermediates such as OD[†].

Vibrationally excited OD[†] can disappear by two side reactions.

- (i) The reactions of OD[†] with O₃ are fast as has been shown for OH[†] by Potter et al.⁽¹⁰⁾
- (ii) The reaction of OD[†] may also be rapid if vibrational energy is useful in surmounting the activation energy of the reaction.

A recent measurement⁽¹¹⁾ of the rate of deactivation of CO₂(v₃) by ozone has shown the process to be highly efficient with a rate constant of $7 \times 10^{11} \text{ cm}^3 \text{ mole}^{-1} \text{ sec}^{-1}$ at 300°K. The high concentration of CO₂ necessary for optimum operation at first seems surprising since it also leads to an initially high concentration of the lower laser state. However the high concentration is obviously necessary to make the OD[†]-CO₂ transfer rate competitive with the unwanted OD[†] side reactions.

The reduction in laser power when H₂ is substituted for D₂ is to be expected on the basis of slower deactivation rates of OD[†] compared with OH[†]. The side reactions of OH[†] may also be faster than OD[†].

Addition of CO was not beneficial to the laser operation. The purpose of the CO addition was to see if the production of OD[†] could be increased by the reaction sequence



However, the rate of the first step cannot compete with the deactivation of $\text{O}(^1\text{D})$ as in $\text{CO} + \text{O}(^1\text{D}) \rightarrow \text{CO} + \text{O}(^3\text{P})$.

The N_2O chemistry is quite similar to the CO_2 chemistry. The only major difference is that the deactivation of $\text{O}(^1\text{D})$ by N_2O leads to N_2 and O_2 .⁽⁵⁾

REFERENCES

1. H.L. Chen, J.C. Stephenson and C.B. Moore, Chem. Phys. Lett. 2, 593 (1968).
2. R.W.F. Gross, J. Chem. Phys. 50, 1889 (1969).
3. J.R. Airey, 3rd Conference on Chemical and Molecular Lasers, May 1972, St. Louis, Missouri.
4. K. Gilpin, H.I. Schiff, and K.H. Welge, J. Chem. Phys. 55, 1087 (1971).
5. F.D. Findlay and D.R. Snelling, J. Chem. Phys. 55, 545 (1971) and J. Chem. Phys. 54, 2750 (1971).
6. R.A. Young, G. Black and T. G. Slanger, J. Chem. Phys. 49, 4758 (1968).
7. P.E. Charters, R.G. MacDonald and J.C. Polanyi, Appl. Optics 10, 1747 (1971).
8. L.F. Phillips and H.I. Schiff, J. Chem. Phys. 37, 1233 (1962).
9. (a) R.R. Stephens and T.A. Cool, J. Chem. Phys. 56, 5863 (1972).
(b) J.R. Airey and I.W.M. Smith, J. Chem. Phys. 57, 1669 (1972).
10. A.E. Potter, Jr., R.N. Coltharp and S.D. Worley, J. Chem. Phys. 54, 992 (1971).
11. J.R. Airey and T.A. Cool, private communication.

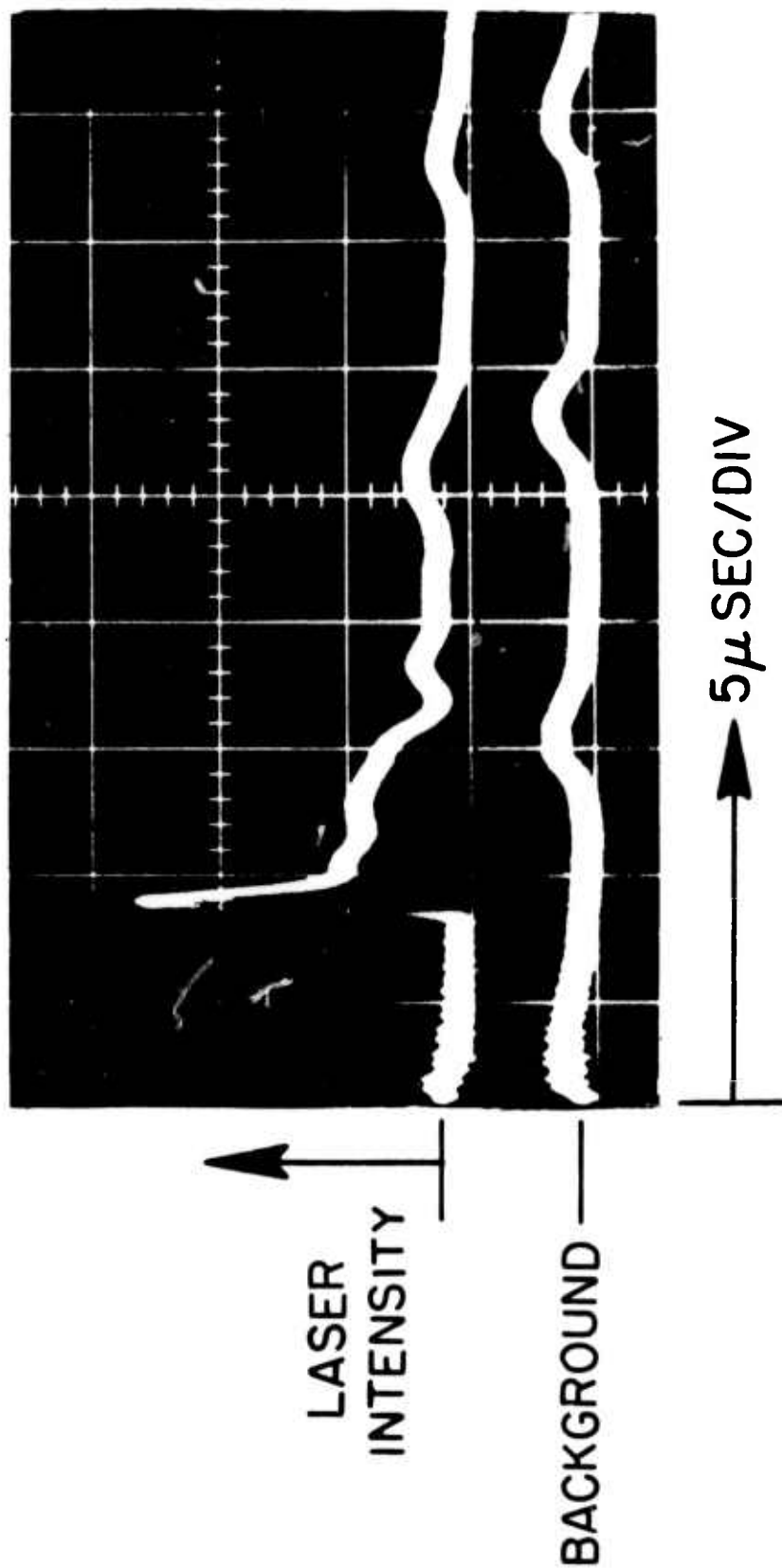


Fig. 1 - Laser emission with background (upper trace) and background (lower trace).

APPENDIX B

A GLASS DISK LASER AMPLIFIER*

J.M. McMahon, J.L. Emmett[†], J.F. Holzrichter[†] and J.B. Trenholme[†]

Naval Research Laboratory
Washington, D.C. 20375

ABSTRACT

This paper is concerned with the details of the analysis, design, and operation of a Nd-glass-disk laser-amplifier which has been constructed at the Naval Research Laboratory. Gain and fluorescence measurements have been compared to theoretical predictions; these show that 0.6 J/cm^3 energy storage is achieved in the disk (assuming a cross section of $3.0 \times 10^{-20} \text{ cm}^2$). The effects of unsuppressed parasitic oscillations are demonstrated, and an effective method of preventing their occurrence is shown. The disk amplifier has demonstrated 320 J output in a 1 nsec pulse with 110 J input.

* Work supported by Advanced Research Projects Agency

[†] Present Address: Lawrence Livermore Laboratory, P.O. Box 808, L-211
Livermore, California 94550

I. INTRODUCTION

High energy, short-pulse lasers are presently of great interest for experiments with plasmas, x-rays and controlled fusion. The designer who contemplates the construction of these systems is presented with major engineering problems, particularly with the final amplifier. This paper is concerned with the details of the analysis, design, and operation of a glass disk laser amplifier which serves as the output stage of a large laser system.

Historically, solid state lasers have been constructed using rods as the active elements. When the designer turns to larger rods as he strives to increase laser output, he finds that the rod fabrication rapidly becomes more difficult as the size increases. In addition, the thermal relaxation time of the rod becomes large, the pump uniformity is poor, and self-focusing of the laser beam in the long path through the rod causes destructive damage. These problems combine to make Nd^{3+} glass rod amplifiers undesirable above a diameter of about 4 cm.

The disk laser⁽¹⁾, in which the active material is in the form of separate slabs set at Brewster's angle to the beam, offers an attractive means of avoiding the problems that beset large rod systems. This was first discussed by Swain et al⁽²⁾. Disks may be made in sizes sufficient to amplify beams much larger than those practical with rods. Fabrication of the disks is relatively easy, and since the disks can be pumped through their faces, pumping uniformity is greatly improved. Damage to one disk due to self-focusing or other causes does not destroy the entire amplifier. Also, rapid thermal transport through the disk faces reduces the thermal time constant compared to a rod of equivalent aperture size (for diameters much greater than the disk thickness).

Disk lasers are not without their own set of problems. The lower average density of active material in a disk amplifier cavity may reduce the pump coupling efficiency, and the long gain paths available in the individual disks may lead to parasitic oscillation problems, although parasitic problems arise in any laser medium when the gain across a characteristic dimension is large. A disk laser will be more complicated (and thus more costly) than a rod laser. Finally, an important practical difficulty is the problem of keeping the many optical surfaces in a disk amplifier clean.

In the following sections, gain and fluorescence measurements on the Naval Research Laboratory's disk amplifier are presented. The results of these measurements are compared to theoretical predictions. We show that a relatively high pumping efficiency has been achieved. The effects of unsuppressed parasitic oscillations are demonstrated, and an effective method of preventing their occurrence is shown.

II. THE NRL DISK LASER

A disk laser amplifier has been constructed and operated at the Naval Research Laboratory. This laser is designed to act as the final amplifier following a modified CGE VD-640 Nd^{3+} glass rod laser system⁽³⁾. The output of the rod system is a 100 J pulse of less than 1 ns duration in a 6 cm diameter beam. The beam profile is not an exact Gaussian, but it has a smooth variation of power with radius, and only small amplitude ripples due to diffraction (this lack of abrupt spatial changes in amplitude is necessary to avoid self-focusing damage in the system). The disk amplifier was designed to have an output of 400 J with this input pulse.

Since the terminal level of the laser transition in laser glass does not have time to empty during a subnanosecond pulse, a maximum of half of the stored energy can be extracted in a single-pass amplifier. The input energy density to the disk amplifier is close to one saturation flux, thus less than this maximum will be extracted. To raise the 100 J input to 400 J means that 300 J must be extracted or that about 1000 J must be stored in the disk amplifier. Measurements by Swain⁽²⁾ et al and preliminary coupling efficiency estimates that 0.6 J/cm^2 could be stored in the glass indicated that $\sim 1700 \text{ cm}^3$ of glass would be required. These considerations led to a design consisting of 11 disks of Owens-Illinois ED-2 glass set at Brewster's angle. Each disk is a 14 cm x 7 cm ellipse of 2 cm thickness. The beam path length through the disks is thus 26 cm.

The pump source for the disks consists of 22 linear flashlamps with their axes parallel to the beam axis. The flashlamps are placed around the disks in a close coupled arrangement (Fig. 1). The lamps have a 145 cm arc length, and are 10 mm ID by 14 mm OD xenon lamps of conventional design filled to 450 T. Each lamp is driven by a separate 42 μF , 20 kV capacitor module through a 300 μH inductor. These circuit values are chosen⁽⁴⁾ to give a critically-damped pulse whose width (340 μs) is optimal for pumping ED-2 glass, and to insure a lamp life of more than 10^4 shots in free air (the lifetime is reduced in the laser cavity due to self loading). The total stored energy in all the modules is 185,000 J at 20 kV.

The cavity structure consists of 11 disk-lamp holders and a two-piece outer reflector (Fig. 1). The metal surfaces were gold-plated to provide high pump-band reflectivity, low uv reflectivity, and chemical inertness in a high-light-flux environment. The cavity is purged with gaseous nitrogen to cool the disks between shots and to remove oxygen from the cavity in order to prevent shock wave formation⁽⁵⁾.

The operation of large laser systems is limited by optical damage caused by the intense optical beam. For pulse widths of several

nanoseconds or less, self-focusing damage is more serious than surface or bulk damage. The flux levels at which our system operates do not exceed the surface and bulk damage thresholds of the glass used. We have observed that self-focusing damage is due to wavefront distortion arising from dirt or optical imperfections, rather than collapse of the beam as a whole.

III. ENERGY STORAGE MEASUREMENTS

When the disk laser was first operated, the gain achieved at high pump levels was considerably less than expected. This difficulty was traced to the presence of parasitic oscillations (free lasing) within the individual disks. These parasitics were eliminated by coating the disk edge with an absorbing glass coating. The disk amplifier was then able to meet the design goal of 0.6 J cm^{-3} energy storage.

The disk laser problem was diagnosed by measuring the small signal gain of the amplifier. For small signals, the amplifier output intensity is given by

$$I = I_0 \exp (\sigma n l - \gamma l)$$

where I_0 is the input intensity, σ is the stimulated emission cross section of the laser material at the signal wavelength ($3 \times 10^{-20} \text{ cm}^2$ for ED-2 at 1.064μ), n is the inversion density, l is the length through the amplifying material (26 cm in this case), and γ is the absorption coefficient. By measuring the pumped and unpumped gain (loss), n may be determined if σl is the same in both cases. The stored energy density is then found from n .

The gain measurements were made using a Chromatix 1000 C $\text{Nd}^{3+}:\text{YAG}$ laser operating in a TEM₀₀ spatial mode as a probe source (Fig. 2). This laser was tuned to the desired transition, and the beam was passed through the disk amplifier. The beam was about 5 mm in diameter, and passed along a line about 2 cm from the center of the disks. A portion of the beam was split off before passage through the amplifier for use as a reference. The reference beam and the amplified beam was measured by Si biplanar photodiodes⁽⁶⁾ with diffusers and pump light shields. Saturation at the detectors was carefully avoided. The probe laser was operated in the pulsed, multiply-Q-switched mode. It emitted six to ten pulses at 20 μsec intervals. The time variation of the disk amplifier gain could thus be followed.

Measurements were first performed to determine if the low gain observed in the disk amplifier was due to a pump-induced loss (that is, to an increase of γ during the pump pulse). Such a loss might be due

to formation of transient color centers in the glass⁽⁷⁾, to an induced absorption in the air path, to pumped birefringence in the disks, or to other unknown causes. However, measurements at 0.946 μm and 1.12 μm showed neither gain nor loss, and measurements at 1.052 μ , 1.064 μ , 1.074 μ and 1.079 μ showed small gains which were proportional to the values of σ at those wavelengths which could be inferred from published fluorescence data on this glass⁽⁸⁾. Thus any pump-induced loss was required to have exactly the same line shape as the gain. This appeared unlikely, and so an induced loss was rejected as the cause of the trouble.

Consequently the difficulty had to be a result of low inversion, which could be due either to fluorescence amplification or to parasitic oscillations. Calculations (outlined later) show that fluorescence amplification causes only a small decrease in inversion for the disk size and gain used in the NRL laser. Thus parasitic oscillations in the disks were the suspected cause.

Parasitic oscillations in disks are expected to be sensitive to the absorption at the disk edge. A series of tests were therefore run with different edge treatments on the disks. For each treatment, a series of measurements were made at different input energies to the disk amplifier. At each energy, the gain was found as a function of time during the disk pump pulse. Figure 3 shows a typical set of these experimental curves, plotted as per disk gain versus time.

The effect of different edge treatments is shown in Fig. 4. This shows the maximum stored energy density achieved as a function of bank energy. A fine-ground, acid-etched surface next to a gold plated surface begins oscillating at an extremely low stored energy of 0.15 J/cm³. Since no more energy may be stored once oscillation starts, the stored energy is limited to a very low value. Replacing the gold surface with blackened copper raises the threshold to 0.43 J/cm³, but oscillation still occurs. When the edge of the disk is coated with a black glass⁽⁹⁾, no oscillation is observed and the desired energy density is achieved. The observed dependence of maximum stored energy on edge treatment shows conclusively that the low gain of the disk laser was caused by parasitic oscillation.

Additional measurements were performed to verify the presence of parasitic oscillations in the disk. The 1.06 μm radiation out of the major and minor axes of one of the elliptical disks was monitored by means of a fiber-optic light guide leading to a monochromator and a S1 photo-multiplier. Small flats were polished on the edges of the disk, and the fiber bundle was optically contacted to one or the other with a high-viscosity silicone fluid. The disk was pumped in its normal position inside the disk amplifier. Neutral density and band-pass filters were required in addition to the monochromator, in order

to maintain linearity and reject flashlamp radiation. Electric and magnetic shielding of the electronics was also employed.

The peak $1.06\ \mu\text{m}$ output from the major and minor axes is plotted in Figure 5 as a function of bank energy. The large, rapidly rising signal along the major axis when a fine-ground, acid-etched edge is next to a gold plated surface is evidence for an oscillation in the disk. The smaller, linear output with a black copper surface is interpreted as a normal fluorescence signal.

IV. THEORETICAL ANALYSIS AND COMPARISON WITH EXPERIMENT

The techniques that have been used in the design and analysis of the disk amplifier include an optical power flow analysis of the pumping in the laser head, a calculation of the effect of fluorescence amplification on the achievable inversion, and a determination of the inversion limits set by parasitic oscillations in the disc amplifier. Details of these calculations and comparisons with experiment follow.

The pumping in the disk laser was analyzed using a model of the spectral emission and absorption of the xenon flashlamps⁽¹⁰⁾ and a versatile optical power flow analysis program⁽¹¹⁾. The physical details of the lamps, disks and disk-lamp support structures were modeled in detail, using the capability of the power flow program to accept complicated, varied geometries. The optical rays which are followed through the laser structure were started uniformly at random, throughout the lamp volumes. Each ray carried spectral power data corresponding to two hundred wavelength intervals from $2000\ \text{\AA}$ to $1.2\ \mu$. The initial power in each interval was set to correspond to the xenon plasma emission at the interval's center wavelength. The ray was then followed through the laser geometry. The ability to treat each wavelength interval separately allowed the wavelength dependent reflectivity of the gold cavity surfaces and the complicated glass absorption spectrum to be treated accurately. The amount of power absorbed by the laser glass, the cavity surfaces, and the lamp plasma was thus found. Since the flashlamps absorb part of their own radiation, both before and after its passage into the cavity, it was necessary to make separate calculations to determine the initial absorption of the rays before they leave the lamps and the subsequent absorption of the rays as they pass through the lamps, glass, etc. The initial internal absorption was found by doing a separate calculation with completely absorbing medium surrounding the lamps. A self-consistent calculation was then used to find the conversion efficiency from electrical power in the lamps to pumping in the glass. The principle of the self-consistent calculation is described in Appendix A. The calculated values of peak inversion as a function of bank energy were fitted to the experimental results by varying the one free variable in the calculation. This variable

called (Q) represents the combined uncertainties in the absorption quantum efficiency, stimulated emission cross section, fluorescent decay in the glass, and inaccuracy in the flashlamp model. Nominal values are assumed for the components of Q , and deviation from these values is reflected in a variation of Q from unity. A factor of 1.06 was also included because the experimentally probed central region of the disks had a higher energy density than the disk average (this factor was found by a power flow calculation in which the disk was divided into a number of small segments). The match for a Q of 0.5 is shown by the solid line in Fig. 4. Agreement is good, but the non-unity value of Q indicates that a problem exists. The absorption quantum efficiency (not to be confused with the fluorescence conversion efficiency) needed to give $Q = 0.5$ is inconsistent with measured values⁽¹²⁾ of unity. A more likely source of the discrepancy is the flashlamp model, which is based on sparse experimental data. The fluorescent decay was modeled by a single 300 μsec decay, which may be wrong. It is also possible that the assumed value of the stimulated emission cross section σ used to relate small signal gain to stored energy density is incorrect ($3.0 \times 10^{-20} \text{ cm}^2$ was used).

The fluorescent loss rate in a laser disk is increased above the normal rate when the gain across a disk is large enough that spontaneously emitted radiation is significantly amplified before it exits from the disk or is absorbed at the edge. This process has been studied in detail⁽¹³⁾ using the same optical power flow program used in the pumping analysis. A negative loss coefficient was used in an elliptical disk to simulate the optical gain of the pumped laser material. A Lorentzian line profile was assumed for the gain, since this gives a reasonable approximation to the more complicated actual line shape. This calculation yielded the nonlinear relation between energy density and loss rate in the disk. The differential equation for the inversion was then integrated, assuming a half-sine pump pulse and the calculated loss rate. The peak inversion resulting from this integration is plotted against the pump energy in Fig. 6 for a pump pulse width equal to the fluorescent lifetime. The point on the curve corresponds to the operation of our laser at peak bank energy. The reduction in peak inversion is only about 0.03 of the peak value in the absence of fluorescence amplification, and thus can be ignored. However, fluorescence amplification arises rapidly as the across-disk gain increases, and therefore may become significant for larger disk lasers.

Lasers are subject to parasitic oscillations if careful measures to suppress the oscillations are not taken. These were first noticed by Swain et al⁽²⁾. Such oscillations arise because of the large gain available in a laser structure. They are harmful because once a parasitic oscillation has begun, no more inversion increase is possible in the oscillating mode volume. This problem has also been analyzed⁽¹³⁾

A simple analysis was used which ignored the effects of phase and diffraction, since these effects will be small in a resonator such as a laser disk which is much larger than a wavelength. The gain along a path such as the one shown in Fig. 7 was calculated as a function of the face and edge intersection angles, assuming uniform gain in the disc. The lowest loss path is the one which lies in a plane across the diameter of the disk, and which hits the faces at the smallest angle from the face normal which still allows total internal reflection. The only losses on such a path come at the edge reflections. At the oscillation threshold this edge loss must just cancel the path gain. Since the path length for this path is the disk refractive index n times the diameter D (assuming the disk is in air), we must have

$$R \exp (nD\alpha) = 1$$

at the oscillation threshold, where α is the gain coefficient in the laser material and R is the edge reflectivity (at the complement of the face angle for total internal reflection). For example, if αD is equal to 3 (i.e., the across-disc gain is 20), and the index is 1.56, then the reflectivity must be less than 1% to avoid oscillation. The most practical method of achieving the required low reflectivities is to coat the edge with an absorbing substance with an index slightly above that of the laser material (an index lower than the laser's allows lossless oscillations near the disk periphery). The reflection will then be due only to the refractive index difference at the disk-coating interface, and thus can be kept small. From a practical standpoint, the coating should match the disk's thermal expansion coefficient (for ease of application), and it should be able to withstand large power loadings. Even if the coating absorbs no pumping radiation, it must absorb about 1/3 of the energy stored in the disk. This loading is due to fluorescent loss, which mostly goes to the disk edge.

The effects of unsuppressed parasitic oscillation are illustrated in Fig. 4. The theory that is given in Ref. 13 indicates that at a certain gain threshold oscillation begins, and the disk gain remains constant. However, the fluorescence that is observed through the disk edges (see Fig. 5) does not show a knee, or threshold point, which would indicate that oscillation had begun. This indicates that the parasitic mode structure in the actual laser disks is somewhat different than that analyzed in the simple mode. In addition, the calculated edge reflectivity that is necessary to cause oscillation at $\alpha l = 0.95$ ($\rho_E = 0.43 \text{ J/cm}^3$) is about 30 - 40%. This is higher than preliminary measurements on the internal smooth ground edge would indicate ($\sim 10\%$). The parasitic model assumed spatially uniform gain

in the disks, which is not the case. An oscillating mode may develop in the heavily pumped face regions of the disk. This mode should not seriously deplete the overall inversion, but it may contribute to the observed large parasitic fluorescence signal. Additional study on the parasitic mode structure and the internal surface reflectivities of laser media is required.

Parasitic oscillation will set a definite upper limit to the size of disk lasers, since oscillation suppression becomes rapidly more difficult as the across-disk gain rises. With present suppression methods, an across-disk gain at the fluorescent line peak of exp (3) probably represents an upper limit. The construction of larger lasers awaits the development of extremely good parasitic suppression methods, or requires some sort of segmenting of the disk to avoid long across-disk paths.

V. DISK AMPLIFIER PERFORMANCE

The disk amplifier was assembled with black edge-coated disks and its performance was tested by using the NRL modified CGE VD-640 laser system as an input source. The output energy as a function of input energy was compared to a theoretical model which is based on a rate equation approach similar to that first formulated by Avizonis and Grotbeck⁽¹⁴⁾. This can be used to predict the output of our amplifier if several assumptions are made:

- (1) the amplifier is a three level amplifier because the lower level decay time is much longer than the pulse duration. The measurements which have been reported all give values for this decay time in excess of 5 nanoseconds⁽¹⁵⁻¹⁸⁾;
- (2) the pulse duration is long compared to T_2^* , the upper level cross relaxation time. From the theoretical treatment of Basov et al⁽¹⁹⁾ and Gobeli et al⁽²⁰⁾ on amplifying ultrashort pulses, one can estimate that T_2 must be shorter than ≈ 30 psec or operation at their reported level would not have been possible.

In this case an equation for the rate of energy addition to the pulse can be derived in the form

$$\frac{dE(Z)}{dZ} = \frac{N}{2} \left\{ 1 - \exp \left(\frac{-2E(Z)}{E_s} \right) \right\} - \gamma E(Z) \quad (1)$$

where $E(Z)$ is the energy density at a given distance Z . N is the upper level energy density (J/cm^3). E_s is the saturation flux, which is equal to $h\nu/\sigma$ and is $\sim 7 \text{ J}/\text{cm}^2$ for the Owens-Illinois ED-2 glass used in the amplifier. γ is the loss coefficient. As has been recently pointed out by Fill and Finckenstein⁽²¹⁾, this equation can be put in the convenient dimensionless form

$$\frac{dE(Z)}{d(\alpha Z)} = \frac{1}{2} \left(1 - \exp(-2E(Z)) \right) - \frac{\gamma}{\beta} E(Z)$$

where $E(Z) = E(Z)/E_s$ and $\beta = \alpha N/h\nu$.

For input energies of up to 75 J, using values of gain (derived from the small-signal experiments) equal to $7.3 \times 10^{-2} \text{ cm}^{-1}$ and $8.4 \times 10^{-2} \text{ cm}^{-1}$ and a loss value of $(5 \pm 2) \times 10^{-3} \text{ cm}^{-1}$, (for both 250 psec and 1 nsec pulses), this equation describes the disk amplifier very well (Fig. 8). The loss coefficient of $5 \times 10^{-3} \text{ cm}^{-1}$ (a transmission of 88% overall) was measured both with a low power Nd:YAG laser and with the output from the 64 mm rod amplifier stage. This loss is due mainly to surface scattering, birefringence in the preceding driver stages, and angular misalignment in the disks themselves.

At 100 joules input the disk amplifier output was less than expected. The properties of the 64 mm rod source were investigated to account for the reduced disk output, and it was found that a mechanism exists which degrades the coherence and collimation of the beam in the final rod amplifier. Figure 9 shows time-averaged shear plate⁽²²⁾ interferograms of the wavefront for intensities below and above the onset of the effect. The ideal wavefront at the output from the 64 mm rod amplifier is a spherically divergent wave and the lower intensity case (Fig. 9A) shows a reasonable approximation to this. The higher intensity case (20 - 30 GW/cm^2 peak power density) shows gross wavefront distortion (Fig. 9B). Burn patterns at this level showed a divergence so large that it was geometrically impossible for the beam to pass through the disk amplifier. The nature of this beam degradation is not understood. It was observed however that the output beam from the disk amplifier as well behaved at power densities well above those at which the beam from the rod system had become unusable⁽²³⁾.

Energies were measured using large carbon cone calorimeters⁽²⁴⁾ preceded by glass attenuators which reduced the input to the calorimeter to a level at which breakdown in the calorimeter did not occur ($< 50 \text{ mJ}/\text{cm}^2$). The attenuation factor of the filters was checked in a separate experiment. The attenuation was found to remain constant up to $\sim 25 \text{ J}/\text{cm}^2$ where surface breakdown occurred. The estimated accuracy of the energy measurements is $\sim 5\%$.

VI. SUMMARY

The present system has shown that a large disk amplifier can be pumped to an energy density that is comparable to or greater than equivalent diameter rods (the 64 mm rod in the system is pumped to $\sim 0.3 - 0.5 \text{ J/cm}^3$). In addition, the optical quality is excellent, the thermal properties with N_2 gas cooling are equivalent to those of a 64 mm rod which is liquid cooled, and the calculated pumping uniformity shows a gain profile which is smooth to $\pm 10\%$. Methods of analyzing and solving the parasitic oscillation problem within single disks have been given. Additional work on self-focusing in these systems must be done, although small scale self-focusing damage should be no worse a problem than in an equivalent length of solid glass.

APPENDIX A

SELF-CONSISTENT PUMPING CALCULATION

The principle of the self-consistent calculation is illustrated in Fig. 10. The computer code⁽¹¹⁾ operates by tracing the power flow from the lamp terminals to optical radiation.

The electrical input power I and the radiation that is absorbed (both before escape from the lamp and after passage through the cavity and back into the lamp) combine to produce the total power input to the lamp. These sources are assumed to be equivalent. This means we have assumed rapid thermalization of the reabsorbed optical energy and spatial equivalence of the electrical input and the reabsorbed radiation. The total power input is converted into radiation S inside the flashlamp, and heat loss H to the lamp wall. An amount of radiation A is absorbed inside the flashlamp; the remainder $(S-A)$ exits from the lamp. Some of the exiting radiation is lost by absorption in the cavity, some is absorbed by the glass, and some is absorbed by the flashlamps. The power absorbed by the laser glass does not all become useful inversion; a portion is lost as heat in the glass instead of contributing to excitation of the ions (absorption quantum efficiency), and even when an ion is excited a fraction of the pump photon energy is lost due to the energy difference between a pump photon and an emitted laser photon (quantum defect). The ray-tracing optical power flow program automatically calculates the effects of the quantum defect, but quantum efficiency must be added later.

The efficiency we desire is the ratio of the inversion to the electrical input, or $\eta = U/I$. The power flow program yields the radiation starting in the lamps S , the total initial internal lamp

absorption plus the subsequent lamp reabsorption F , the useful inversion U , and (in a separate black-exterior run) the initial lamp internal absorption A . We must find the electrical input I in order to calculate η . We have $I = S + H - F$, where H is the heat lost to the flashlamp. This loss must be found from the radiative efficiency of the flashlamps, which may be determined from the model of xenon flashlamps⁽¹⁰⁾. The radiative efficiency is $R = (S-A)/(S + H - A)$, so

$$H = (S-A) \left(\frac{1}{R} - 1 \right) .$$

Therefore

$$\eta = \frac{UQ}{\frac{S-A}{R} + A - F}$$

where Q is the quantum efficiency (assumed constant with wavelength).

The self-consistent calculation of transfer efficiency is done for a number of input current densities. However, the flashlamp model derives the plasma state from the input current density along, and does not allow for an increased energy input due to radiation reabsorbed from the cavity. It is therefore necessary to reduce the input current density so that the sum of electrical and radiation inputs is equal to the originally assumed electrical input. The electrical input must be reduced from $S + H - A$ to $S + H - F$, or from $(S-A)/(R + A - F)$ to $(S-A)/R$. Since the power goes as the $3/2$ power of the current density⁽⁴⁾, the current density must be reduced from the assumed value by a factor K which is given by

$$K = \left[1 - R \left(\frac{F-A}{S-A} \right) \right]^{2/3} . \quad (1)$$

It should be added here that the lifetime of the flashlamps must be calculated from their total input power, which is equal to the total power density. The self-consistent relationship between transfer efficiency and instantaneous current density is determined by using the procedure described above.

The actual peak inversion in the laser material is determined as follows. An assumed power density in the lamps is multiplied by the transfer efficiency (which can be a function of power density) to find the pumping rate in the glass as a function of time. In practice the transfer efficiency is assumed to be constant, corresponding to a power

density = 0.72 times the peak power density. Calculations have shown this to be a good approximation. This pumping rate is used as the forcing function in the differential equation which describes the decay of the inversion (in general this differential equation should include the effects of fluorescence amplification and parasitic oscillation⁽¹³⁾). The calculation is further simplified by assuming that the spontaneous fluorescence loss reduced the stored inversion to 0.66 of the value it would achieve with zero loss. This value of 0.66 is appropriate for a half-sine pump pulse of base width equal to the fluorescent lifetime of the material (300 μ sec), which is close to the situation in our laser. For this pulse width, a given inversion in the glass is associated with a time integrated power density dissipated in the lamp. The current density which corresponds to this power density must be reduced by the factor K (eqn. 1) to account for the reabsorbed optical power in the lamps. By using the results for a single flashlamp discharge circuit,⁽⁴⁾ one can work backwards from the corrected current density to find the stored capacitor bank energy. An additional 0.08 loss is included to account for the measured capacitor-to-bank transfer loss.

REFERENCES

1. J.C. Almasi, J.P. Chernoch, W.S. Martin, and K. Tomiyasu, "Face Pumped Laser", G.E. Report to ONR, May 1966.
2. J.E. Swain, R.E. Kidder, K. Pettipiece, F. Rainer, E.D. Baird, and B. Loth, "Large-Aperture Glass Disk System", J. Appl. Phys., Vol. 40, pp 3973-3977, September 1969.
3. The disk amplifier was designed to be driven by a modified Compagnie General d'Electricite' Model VD-640 laser system. A specially constructed Nd:YAG mode locked oscillator, pulse switch-out system, and two Nd:YAG preamplifiers provide an 80 mJ pulse, 20 psec to 1 nsec in duration. This pulse is spatially shaped to minimize Fresnel fringing in the glass amplifier system. The glass system amplifies this pulse to the 100 J level (for 1 nsec pulses) and provides a diffraction limited pulse with self phase modulation kept less than a 1.0 cm^{-1} .
4. J.P. Markiewicz and J.L. Emmett, "Design of Flashlamp Driving Circuits", IEEE J. of Quantum Electronics, Vol. QE-2 (11), pp. 707-711, November 1966.
5. R.C. Elton, "A Study of Radiation Induced Shock Waves External to Quartz Discharge Tubes and Associated Fracture Problems", Plasma Physics (Journal of Nuclear Energy, Pt. C), Vol. 6, pp 401-404 (1964).
6. The photodiodes used in these experiments were made by ITT. The model number is FW-4018(S1).
7. E. Snitzer and R. Woodcock, "Saturable Absorption of Color Centers in Nd^{3+} and Nd^{3+} - Yb^{3+} Laser Glass", IEEE J. of Quantum Electronics, Vol. QE-2, pp 627-632, September 1966; and R.J. Landry and E. Snitzer, "Ultraviolet-Induced Transient and Stable Color Centers in Self-Q-Switching Laser Glass", J. Appl. Phys., Vol. 42, pp 3827-3837, September 1971.
8. D.K. Dustin, "Factors Influencing the Gain in Neodymium Doped Laser Glass", M.S. Thesis, Dept. of Elect. Engr., Rensselaer Polytechnic Institute, Troy, New York, 1969 (p. 39).
9. The disk edges were coated with a low melting point, black solder glass developed by Owens-Illinois. The reflectivity at the laser glass coating interface was measured to be 0.25%.

10. J.B. Trenholme and J.L. Emmett, "Xenon Flashlamp Model for Performance Prediction", Proceedings of the 9th International Conference on High Speed Photography, SMPTE, N.Y., 1970 (p. 299).
11. J.H. Alexander, M. Troost, and J.E. Welch, The Zap Laser Analysis Program, Systems, Science and Software Inc., 1971 (available from DDJ as AD-884-920) modified by one of the authors (JBT).
12. L.G. DeShazer and L.G. Komai, "Fluorescence Conversion Efficiency of Neodymium Glass", J. Opt. Soc. Am., Vol. 55, pp. 940-944, August 1965.
13. J.B. Trenholme, "Fluorescence Amplification and Parasitic Oscillation Limitations in Disc Lasers", Naval Research Laboratory Memorandum Report 2480, July 1972.
14. F.W. Avizonis and R.L. Grotbeck, "Experimental and Theoretical Ruby Laser Amplifier Dynamics", J. of Appl. Phys., Vol 37 (2), pp. 687-693, February 1966.
15. J.M. McMahon and T.H. DeRieux, "Laser Glass Testing at NRL" in 2nd ASTM-NBS Symposium on Damage in Laser Materials, NBS Special Technical Publication No. 341, pp 19-27 (December 1970).
16. P.C. Magnante, "Influence of the Lifetime and Degeneracy of the $^4I_{11/2}$ Level on Nd-Glass Amplifiers", IEEE J. of Quantum Electronics, Vol. QE-8 (5), pp 440-448, May 1972.
17. W.E. Hagen, "Diffraction Limited High Radiance Nd-Glass Laser System", J. Appl. Phys., Vol. 40, pp 511-16, February 1969.
18. R. Dumanchin, J.C. Farcy, M. Michon and P. Vincent, "Analysis of Giant Pulse Amplification in Nd^{3+} Doped Glass", IEEE J. Quantum Electronics, Vol. QE-7, pp 53-59, February 1971.
19. N.G. Basov, R.V. Ambartsumyan, V.S. Zuev, P.G. Kyrukov, and V.S. Letokhov, "Nonlinear Amplification of Light Pulses", JETP Vol. 23, pp 16-23, July 1966.
20. G.W. Gobeli, J.C. Bushnell, P.S. Peercy, and E.D. Jones, "Observation of Neutrons Produced by Laser Irradiation of Lithium Deuteride", Phys. Rev., Vol. 188 (1), pp. 300-302, December 1969.
21. E.E. Fill and K. Graf V. Finckenstein, "A Comparison of the Performance of Different Laser Amplifier Media", IEEE J. of

Quantum Electronics, Vol. QE-8, pp 24-26, January 1972.

22. See for instance, M.V.R.K. Murty, "The use of a Single Plane Parallel Plate as a Lateral Shearing Interferometer with a Visible Gas Laser Source" Appl. Optics, Vol. 3(4), pp 531-535, April 1964.
23. Operation of a tilted-slab laser at 50 GW/cm^2 has recently been reported; M.J. Lubin, J.M. Soures, and L.M. Goldman, "Large-Aperture Nd-Glass Laser Amplifier for High-Peak-Power Application," J. Appl. Phys., Vol. 44(1), January 1973.
24. CG-64 calorimeters manufactured by the Compagnie Industrielle des Lasers (CILAS), Marcoussis, France, were used. These are distributed in the U.S. by Hadron, Inc.

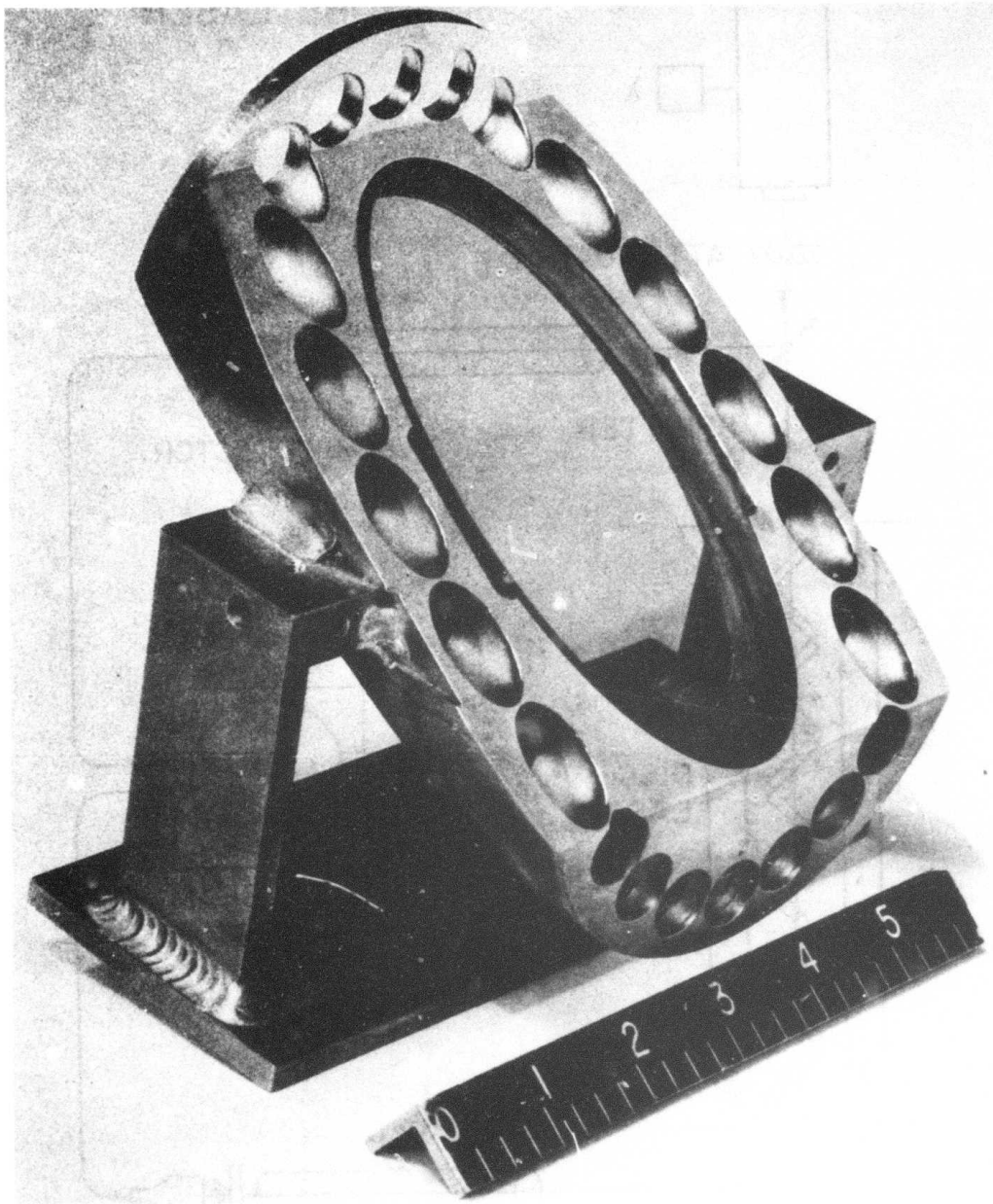


Fig. 1 - Individual disk-lamp holder (scale is in inches). The disk amplifier assembly consists of eleven of these holders placed end to end in a zig-zag pattern. Twenty-two lamps each 60 inches long are slid through the disk holders to completely surround the disks. Separate top and bottom reflectors are placed around the disk holders. All of the metal surfaces are gold plated.

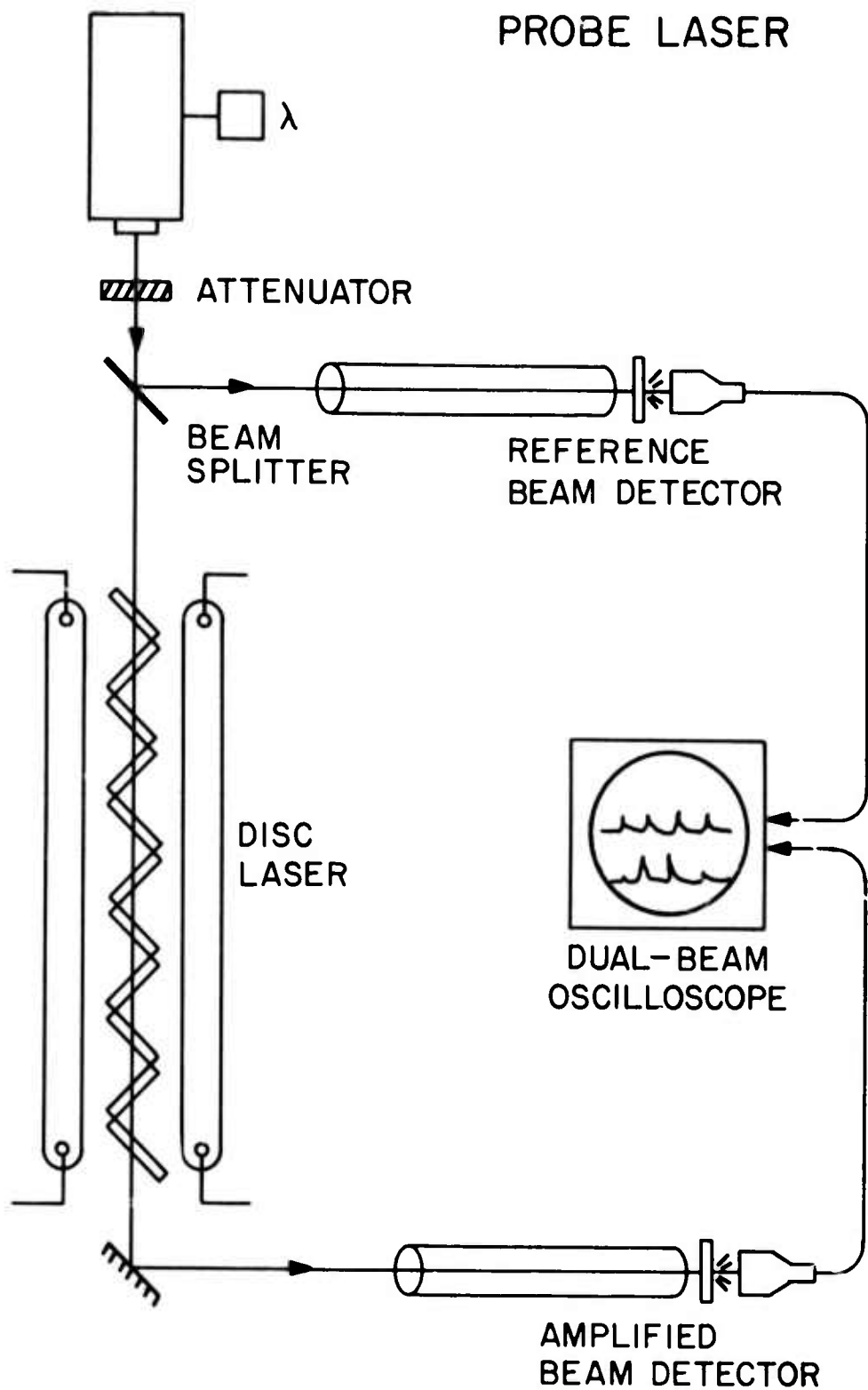


Fig. 2 - Small signal gain measurement setup. A Chromatix 1000 C Nd:YAG laser was used to probe the disk amplifier gain. The wavelength of the probe could be adjusted from 0.96μ to 1.079μ .

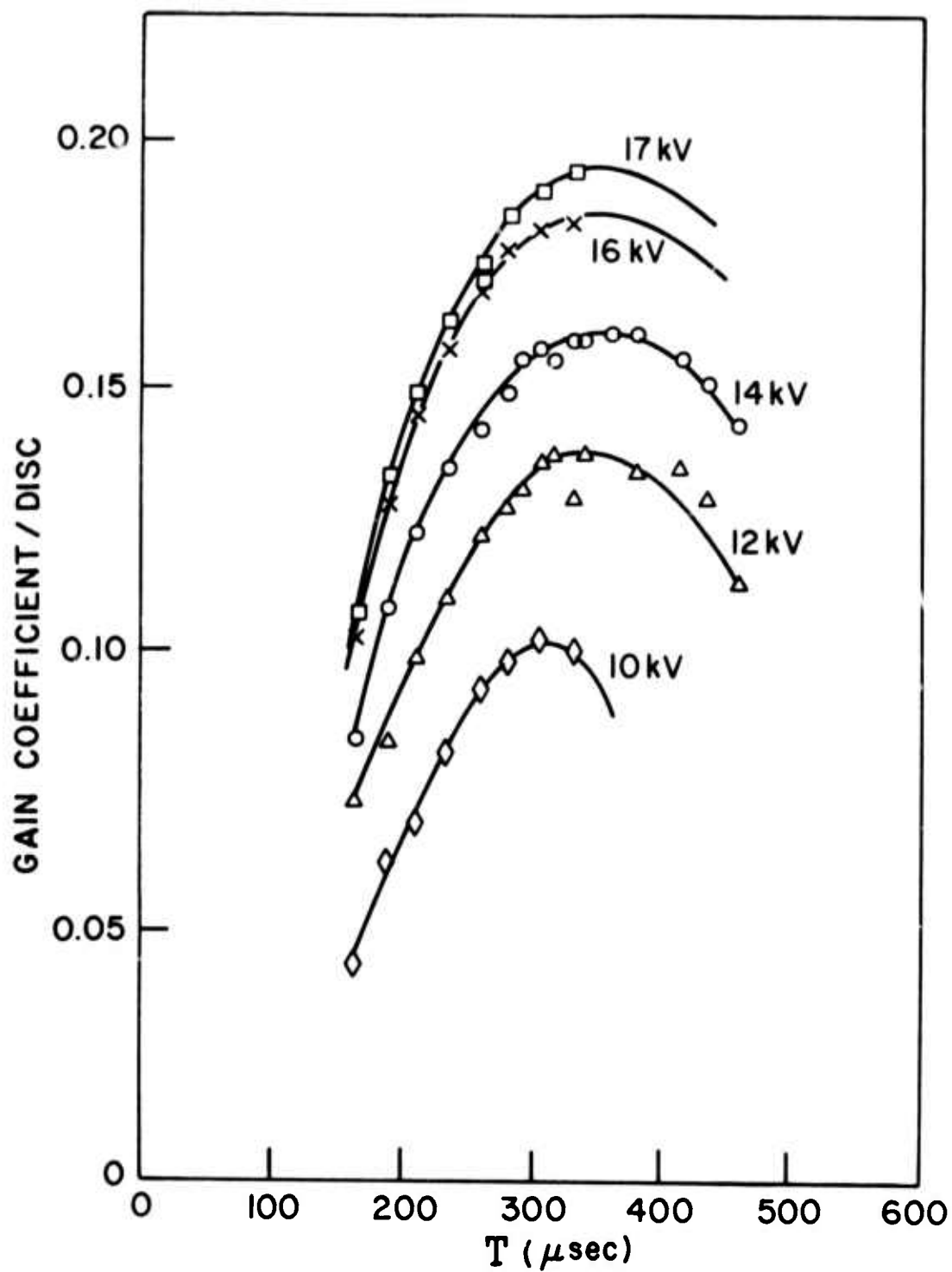


Fig. 3 - Disk gain coefficient as a function of time and bank voltage. Total stored energy in disk amplifier capacitor bank is 185 kJ at 20 kV.

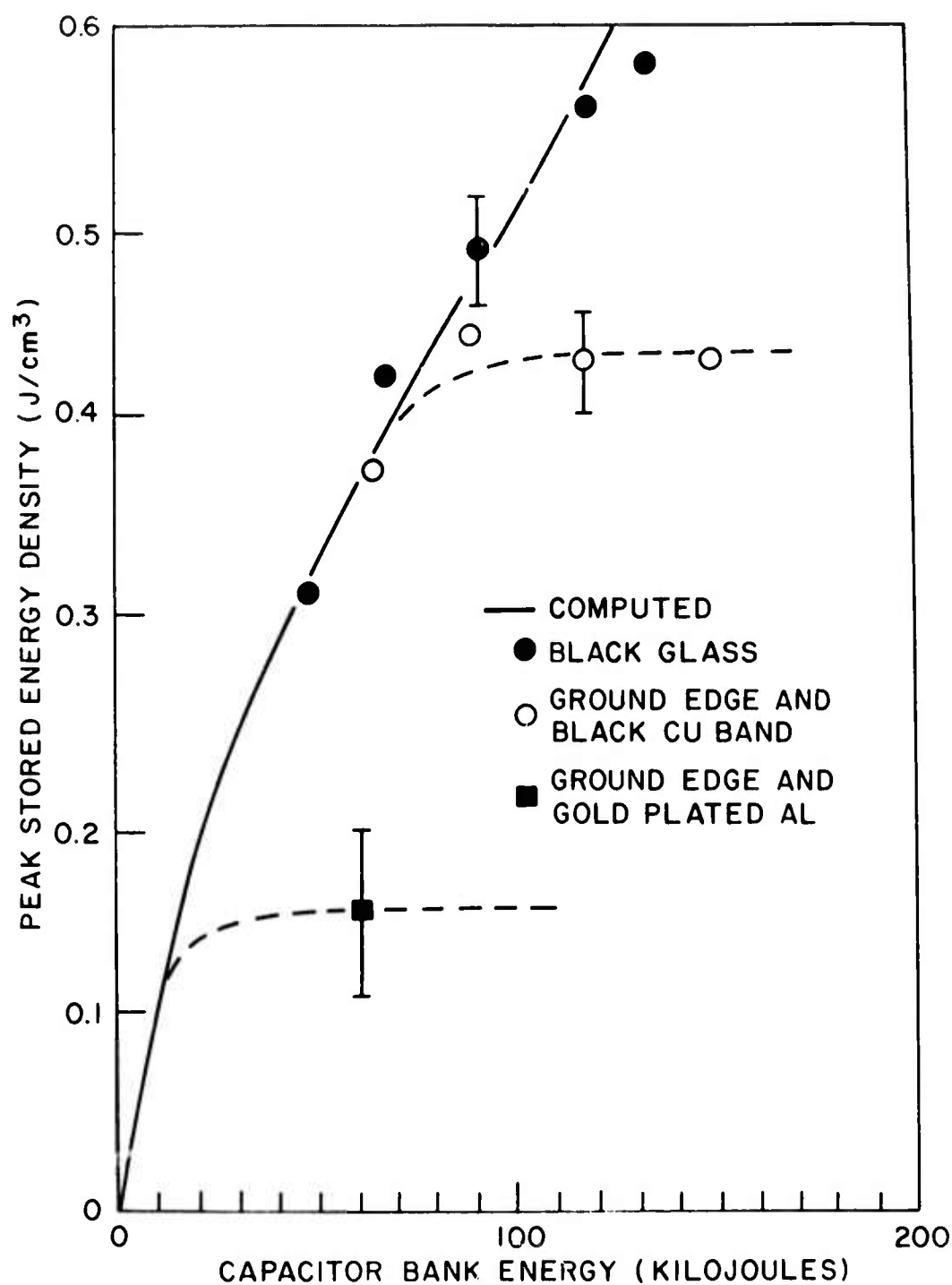


Fig. 4 - Comparison of experimental and calculated energy density in the disk laser. The solid line shown is the calculated energy density in the disks vs flashlamp input energy. The solid round points show the measured energy storage (gain) as a function of bank energy for black edged disks. The open round and solid square points are experimental measurements of gain saturation due to parasitic oscillation in uncoated disks.

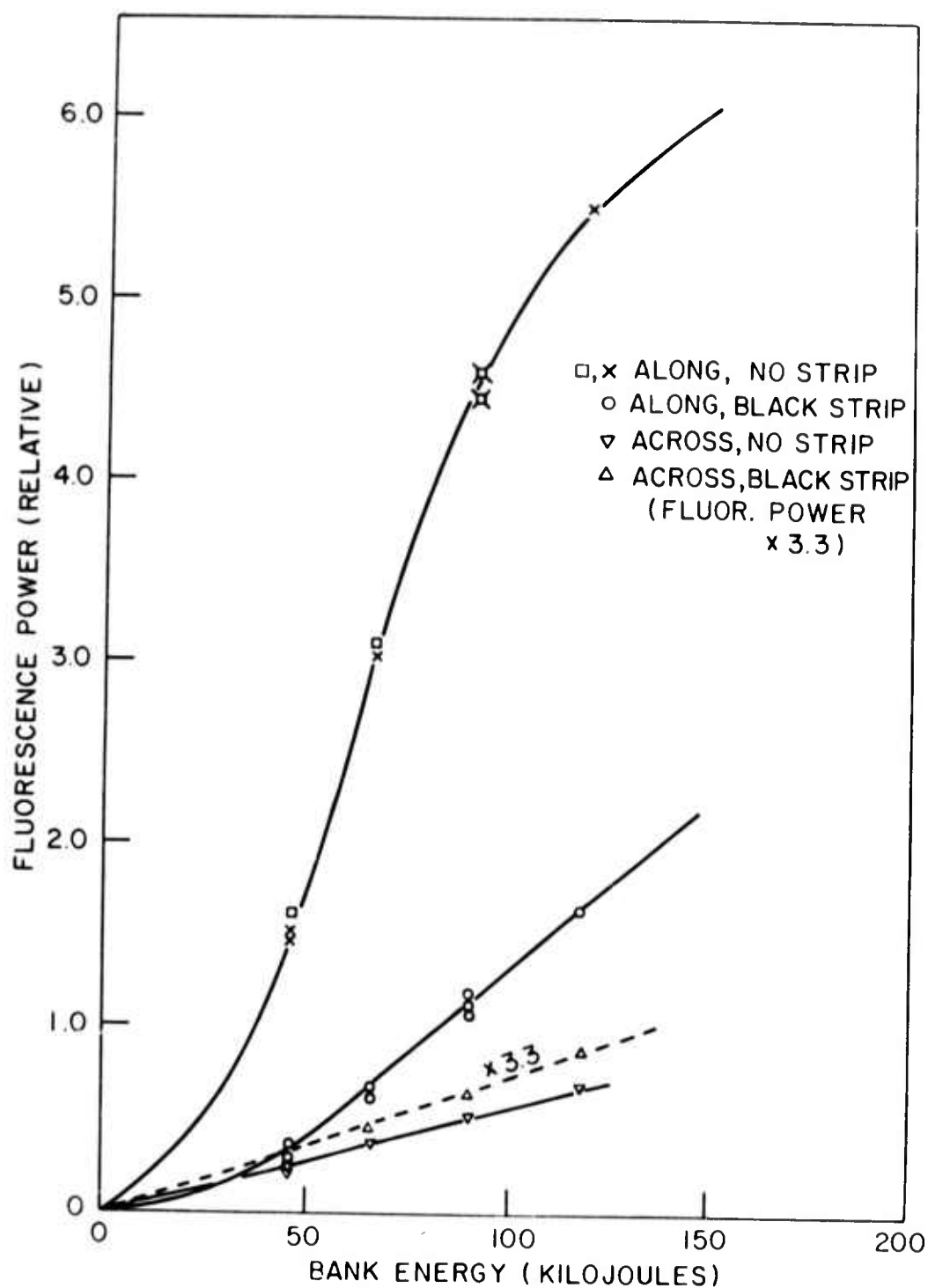


Fig. 5 - Peak fluorescence power through disk edge as a function of edge preparation. Coatings were not applied to the disk edges for the data presented here. Along and across refer to observation direction along the disk major axis or across it (i.e. along the disk minor axis). Notice that the across data taken with the black strip between the disk edge and the holder are magnified by 3.3.

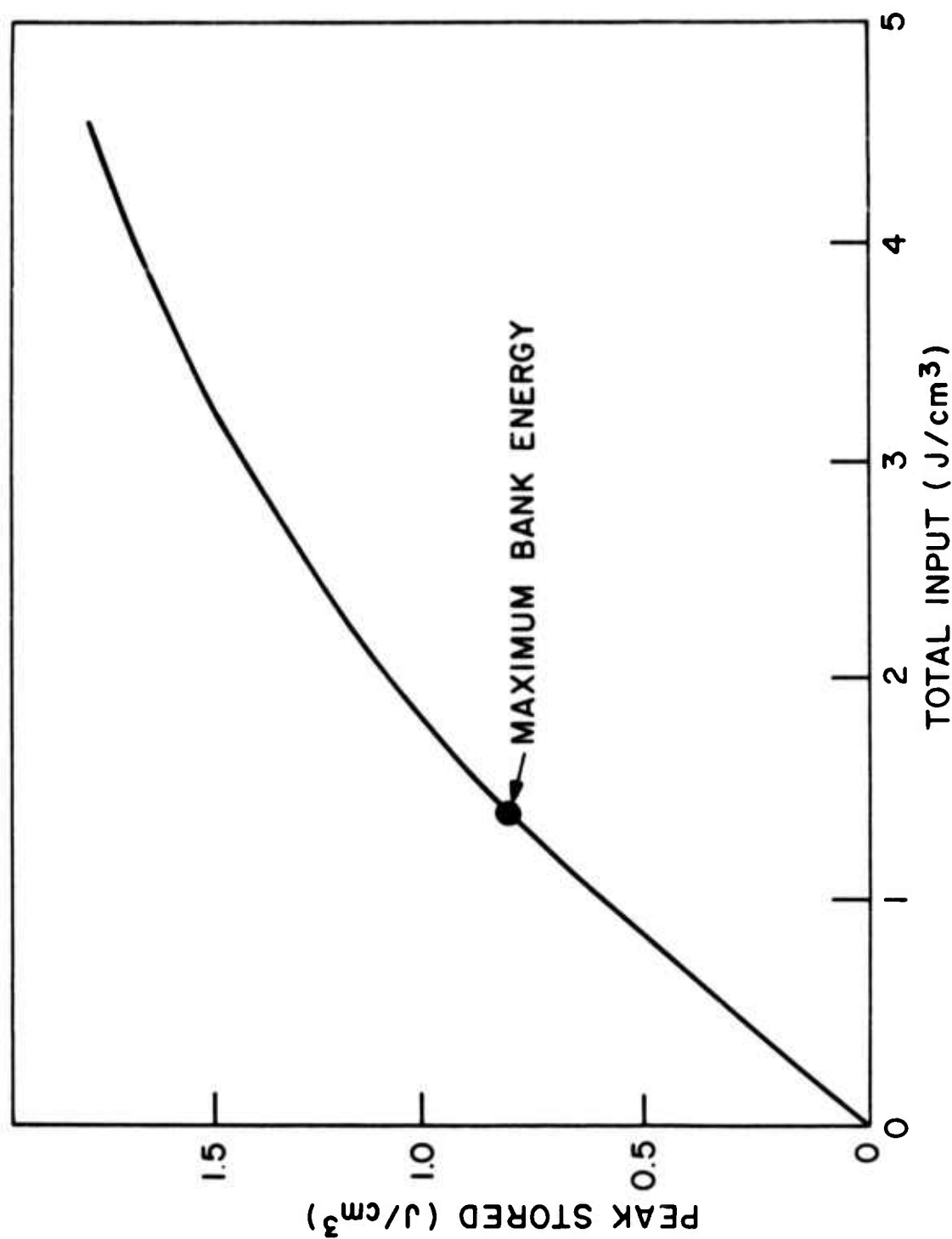


Fig. 6 - Effect of fluorescence amplification on peak stored energy versus total absorbed energy, calculated for a disk similar to that in the NRL amplifier. The reduction is only 3% at the maximum pump energy.

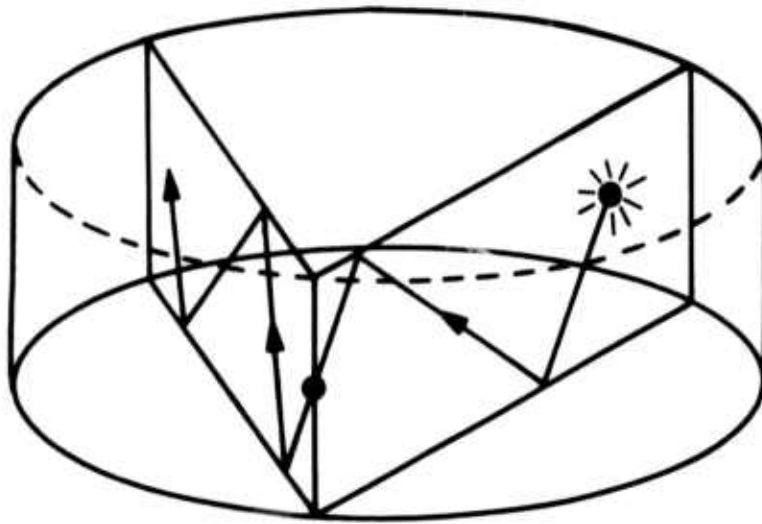


Fig. 7 - Ray path which bounces off both laser disk face and edge. Between edge reflections, the path zig-zags in a plane perpendicular to the faces. The path changes to a new plane at each edge reflection.

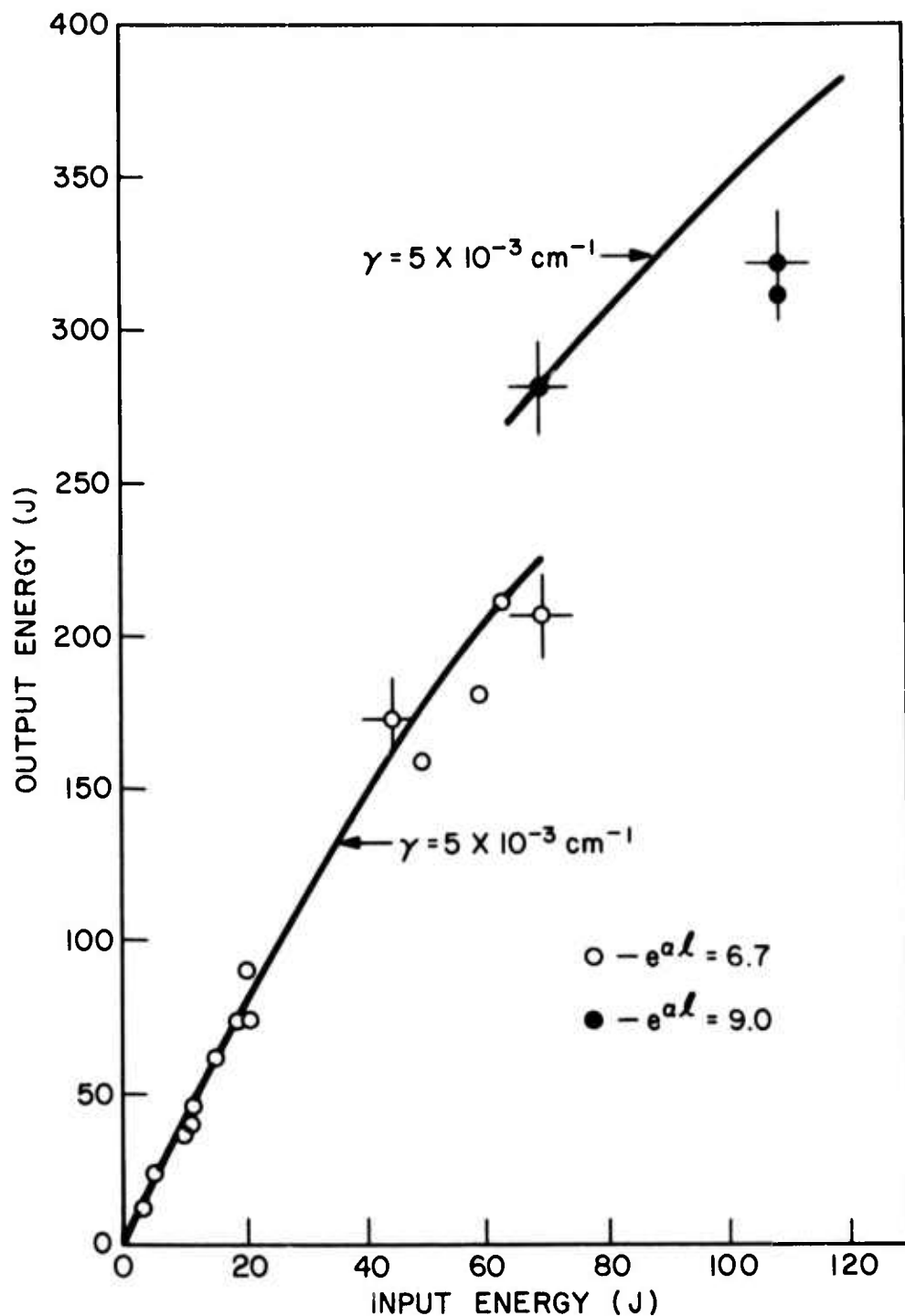
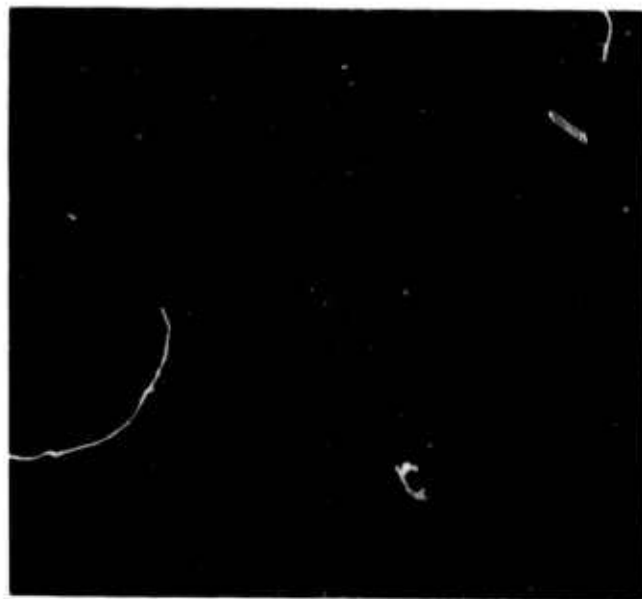


Fig. 8 - Disk output energy as a function of input energy. Both .25 and 1.0 nsec pulses are used as input pulses. Gain values of $\alpha l = 1.9$ and $\alpha l = 2.2$ were used. The loss coefficients γ are explained in the text. At the higher gain level of $\alpha l = 2.2$ with 75 J input energy, the disk performs as expected. At 110 J input, the apparent disk gain falls due to the increased divergence of the input beam.



(a)



(b)

Fig. 9 - Shearing plate interferograms of the output from the 64 mm rod amplifier interferogram (a) shows a nearly spherically diverging beam from the amplifier. This can be corrected with a 8 M focal length lens of yield ≤ 1 wavelength of distortion across the beam. interferogram (b) shows gross wavefront distortion present when the self-focusing threshold is reached. The figures were photographed from burn patterns on exposed and developed copy paper, supplied by Hadron, Inc., 800 Shames Drive. Westbury, N. Y.



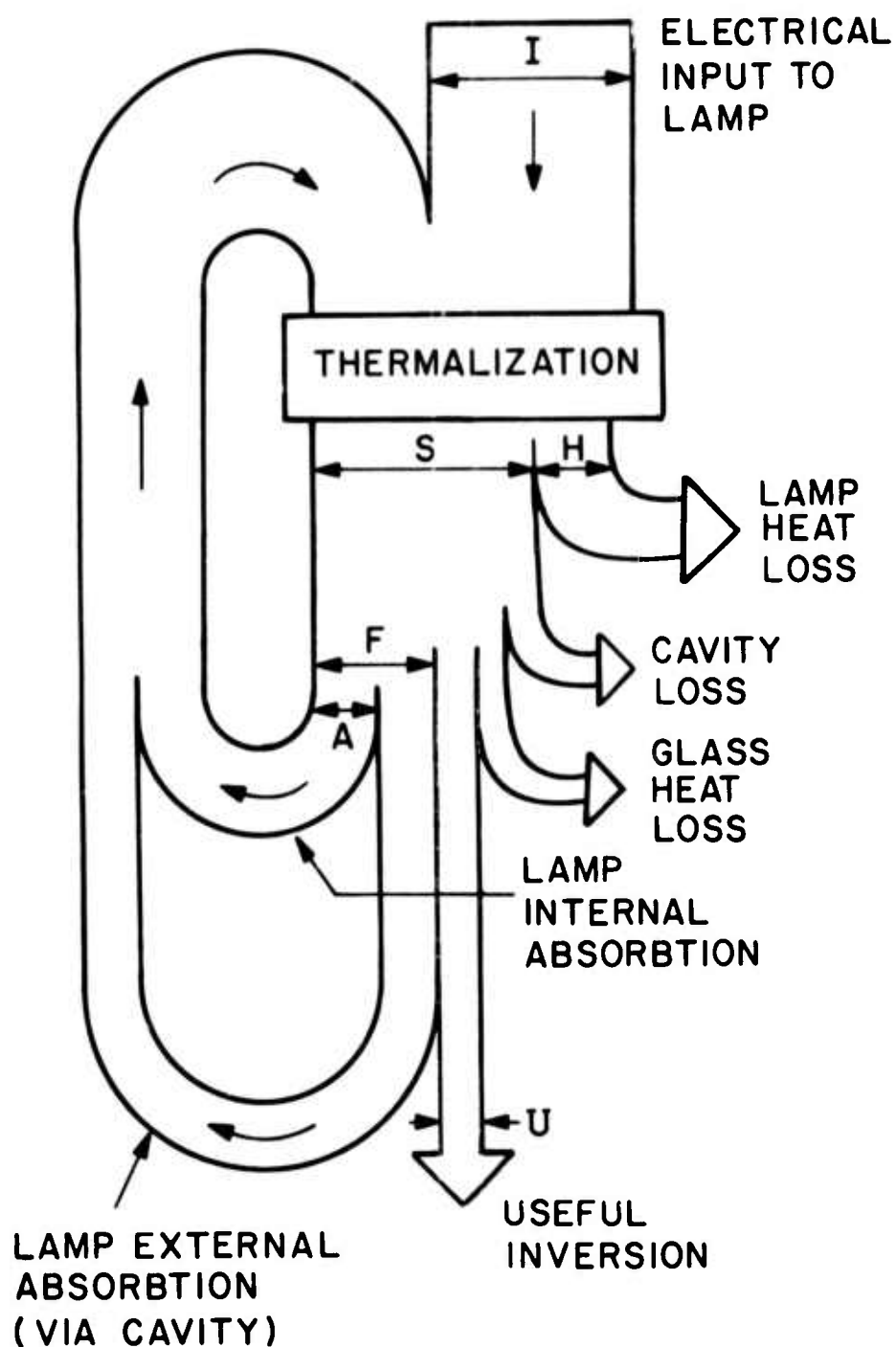


Fig. 10 - Diagram illustrating the flow of power in a laser cavity. The return of power to the lamps after passage through the cavity (lamp external absorption) requires a self-consistent calculation of the electrical-to-inversion transfer. See text for description.

APPENDIX C

DEPENDENCE OF LASER INDUCED BREAKDOWN FIELD

STRENGTH ON PULSE DURATION

D.W. Fradin and N. Bloembergen*
Gordon McKay Laboratory
Harvard University
Cambridge, Mass. 02138

and

J.P. Letellier†
Naval Research Laboratory
Washington, D.C. 20375

ABSTRACT

Fields strengths at which optical damage is initiated in NaCl have been measured with a mode-locked Nd:YAG laser with pulse durations of 15 and 300 picoseconds. Comparison with previously reported data with a Q-switched laser shows that the field strength required for intrinsic optical damage increases by almost one order of magnitude from 10^6 V/cm at 10^{-8} sec to over 10^7 V/cm at 1.5×10^{-11} sec. This is in qualitative agreement with published estimates based on the electron avalanche breakdown mechanism.

* Supported by the Joint Services Electronics Program at Harvard University under Contract No. N00014-67-A-0298-J006 and by the Advanced Research Projects Agency at Raytheon Research Division as monitored by the Air Force Cambridge Research Laboratories under Contract No. F19628-73-C-0127.

† Supported by NRL Problem K03-08.502, ARPA Project Order 2062, Project 62301D.

Damage produced by laser beams of high intensity in transparent materials has been studied intensively for many years. It is only recently, however, that the effects of absorbing inclusions and self-focusing have been carefully eliminated, and the intrinsic breakdown mechanism in transparent condensed dielectric media has been positively identified as electron avalanche ionization¹⁻⁶. On the basis of this mechanism and known characteristics of d.c. breakdown by avalanche ionization, Yablonovitch and Bloembergen³ predicted a characteristic dependence of breakdown field strength on laser pulse duration. In this note an experimental determination of this dependence in the sub-nanosecond regime is presented, which turns out to be in general agreement with those prediction.

The measurements were performed by focusing mode-locked YAG:Nd laser pulses having durations of 15 and 300 picoseconds inside a single crystal of NaCl. Because the experimental procedures used in the present work were identical to those used in recent studies with a Q-switched YAG:Nd laser,⁴ the subnanosecond measurements can be directly compared to the results of these studies. It is found that the intrinsic breakdown field increased by almost an order of magnitude to over 10^7 volts/cm as the laser pulsewidth was decreased from 10 nanoseconds to 15 picoseconds. Previous data with pulse widths typical of Q-switched lasers had demonstrated that the dependence on pulse width in the nanosecond regime is small so that relatively little information on the time dependence of the avalanche process was available.⁷ Our results demonstrate again that lasers can be used to measure properties of dielectric breakdown which are difficult to obtain by d.c. techniques.⁸⁻¹¹

The laser used for the present work was a passively mode-locked YAG:Nd laser operating in a TEM₀₀ mode at 1.06 μ m. Without intercavity etalons, this oscillator produced bandwidth-limited light pulses of 15 picosecond duration. By replacing the output mirror with a sapphire etalon, the pulsewidth was lengthened to about 300 picoseconds. Two-photon fluorescence measurements failed to detect substructure with pulses of either duration. A laser-triggered spark gap¹² was used to select a single light pulse which, after attenuation, was focused through a 15-mm focal length lens about 2 mm into the sample. Care was taken to insure that spherical aberrations from both the lens and the plane entrance surface of the sample being tested were unimportant. An energy monitor recorded the energy in each laser pulse.

The intrinsic damage process is statistical in nature^{2,6} because of the fluctuations in the formation of the first few hot electrons in the small focal volume (about 10^{-7} cm³). The damage threshold can be defined as that value of the r.m.s. electric field inside the sample which produces damage during one pulse with a probability of 0.5.

In NaCl the threshold is quite sharp and damage was identified by the occurrence of a faint spark and concomitant melting of a small region ($\sim 2 \times 10^{-9} \text{ cm}^3$) inside the crystal. At least 20 data points were taken at each pulse duration at the 0.5 probability point.

Beam distortion from self-focusing was avoided by confining the laser input powers to well below the calculated critical powers for catastrophic self-focusing.⁴ (See Table I). To verify the absence of self-focusing, two different lenses (focal lengths of 15 mm and 25 mm) were used to focus the laser radiation. As expected from diffraction effects alone, the input damage powers scaled with the square of the focal lengths. If catastrophic self-focusing had been present with the subnanosecond pulses, the input damage power would have been independent of focal length.⁴

A number of tests have been developed to distinguish between damage from absorbing inclusions and damage from intrinsic breakdown.^{1,6} Two of these tests - examination of the damage morphology and examination of the transmitted laser light - could not be used in the present work because of the small volumes of the damaged sites and the short durations of the laser pulses. But because breakdown is virtually threshold-like in NaCl, other tests were possible. It was observed that the damage field was well defined and did not change as different regions of the sample were probed and lenses with different focal lengths were used to focus the radiation. Also, only one spark occurred with each damaging laser pulse, and the spark always appeared to form at the geometrical focal plane. These observations contrasted with those obtained under conditions where inclusion damage was seen.⁵ It was therefore concluded that except possibly for occasional damage sites, inclusion damage was absent in highly pure NaCl under the conditions of our measurement as it had been in previous work⁴ where Q-switched lasers were used.

Table I summarizes the results of the present measurements and those of Ref. 4. An increase in breakdown strength was observed as the duration of the laser pulse was decreased. As the pulse duration was changed from 10.3 ns to 15 ps, there was a total change by a factor of 5.8 in damage field strengths or a factor of 33 in damage intensity. The experimental points are plotted in Fig. 1, together with some semi-empirical predicted curves taken from Ref. 3.

In the subnanosecond regime electron diffusion and self-trapping may be ignored. The density of the conduction electrons in the avalanche changes exponentially with time,

$$N(t) = N_0 \exp \left[\int \alpha(E) dt \right] = N_0 M_c(t) \quad . \quad (1)$$

When the electron density exceeds about 10^{18} cm^{-3} , requiring a multiplication factor of roughly $M_c \sim 10^8$, breakdown is said to occur. According to Eq. (1) the ionization rate $\alpha(E)_{\text{rms}}$ is related to the pulse duration as follows:

$$\alpha(E_{\text{rms}}) = t_p^{-1} \ln M_c \approx 18 t_p^{-1}. \quad (2)$$

This relation has been used to convert the quantity $\alpha(E)$ used along the vertical axis in the figure of Ref. 3 to our figure which uses t_p^{-1} . We have shifted the curves along the horizontal axis to obtain agreement with the experimental values for the breakdown field E_{rms} for the long pulses. It should be noted that the d.c. breakdown fields quoted in references 8-10, on which the curves in Ref. 3 were based, are about a factor 2.3 lower than our laser values for E_{rms} . There are reasons to suspect that this factor is due to systematic errors in the d.c. experiment. First, this factor of 2.3 is nearly the same for all nine alkali halides studied at $10.6 \mu\text{m}^3$ and $1.06 \mu\text{m}$,⁴ and second, d.c. field values are average values without regard for field inhomogeneities from space charge effects which can be important in d.c. experiments.^{13,14} Consistent with the approach of Ref. 1 and 4, it is therefore more meaningful to compare trends in breakdown fields as different materials are investigated or as parameters are varied then to compare the absolute values of breakdown fields.

It is seen that the experimental points fall close to the upper curve of Ref. 3, which was derived on the assumption that the mobility in the hot electron gas is independent of E_{rms} . Quantitative agreement should not be emphasized, however, because the analysis is based on assumptions which are questionable over the range of damage fields considered. As mentioned before, space charge and electrode effect may considerably alter the interpretation of the d.c. results⁸⁻¹¹ and consequently to transition from E_{dc} to E_{rms} along the horizontal axis. Furthermore the breakdown field at the shortest pulse durations becomes so high that it is possible that frequency-dependent tunneling (for multiphoton ionization) takes over as an intrinsic damage mechanism. In Ref. 3 it was estimated that this change over would occur for fields higher than $2 \times 10^7 \text{ V/cm}$ or pulse durations shorter than one picosecond. If this estimate is inaccurate and this other intrinsic breakdown mechanism begins to compete with avalanche ionization, the trend would be to push the experimental points upward and to the left of the prediction curves based on the avalanche effect alone.

In summary, intrinsic laser-induced damage has been shown to be a time-dependent process. As the laser pulsewidth was decreased to 15 ps,

the damage field in NaCl increased to over 10^7 V/cm. From the pulse-width dependence of the optical damage field, a field-dependent ionization rate was determined and found to agree at least qualitatively with experiments using d.c. fields. The agreement underscores the basic similarity between intrinsic laser-induced damage at $1.06 \mu\text{m}$ and d.c. dielectric breakdown and adds further support to the existence of avalanche ionization in self-focusing "filaments", where effects also occur on a picosecond time scale.

We wish to thank M. Bass, L. Holway, E. Yablonovitch and J.M. McMahon for numerous helpful discussions. M. Bass and J.M. McMahon were particularly helpful in establishing arrangements for this work.

REFERENCES

1. E. Yablonovitch, Appl. Phys. Letters 19, 495 (1971).
2. M. Bass and H.H. Barrett, IEEE J. of Quantum Elect. QE-8, 338 (1972).
3. E. Yablonovitch and N. Bloembergen, Phys. Rev. Lett. 29, 907 (1972).
4. D.W. Fradin, E. Yablonovitch, M. Bass, Appl. Opt. 12 (April 1973).
5. D.W. Fradin and M. Bass, Appl. Phys. Lett. 22 (1 March 1973).
6. M. Bass and D.W. Fradin, IEEE J. of Quantum Elect., submitted for publication. See also, D.W. Fradin and M. Bass, Appl. Phys. Lett. 22 (15 February 1973).
7. A pulsewidth dependence to optical damage in thin films was first observed by E.S. Bliss and D. Milam, 4th ASTM Symp. on Damage in Laser Materials, NBS Spec. Pub. 372, 108 (1972).

The mechanism of damage was not identified, however. Since it is known that thin films can have a large residual absorption and significant structural defects and that both effects can change the damage characteristics of surfaces, it is not clear that the change in damage fields which were observed by Bliss and Milam reflect a property of an intrinsic bulk damage mechanism.
8. A.A. Vorob'ev, G.A. Vorob'ev, and L.T. Musashko, Fiz. Tverd. Tela 4, 1967 (1962) [Soviet Phys. Solid State 4, 1441 (1963)].
9. D.B. Watson, W. Heyes, K.C. Kao, and J.H. Calderwood, IEEE Trans. Elec. Insul. 1, 30 (1965).

10. G.A. Vorob'ev, N.I. Lebedeva, and G.S. Nadorova, Fiz. Tverd. Tela 13, 890 (1971) [Sov. Phys. Solid State 13, 736 (1971)].
11. J.J. D'Dwyer, The Theory of the Dielectric Breakdown of Solids, (Oxford Press, London, 1964).
12. J.P. Letellier, Naval Research Laboratory Report 7463 (1972).
13. H. Raether, Electron Avalanches and Breakdown in Gases (Butterworths, London, 1964), See also J.R. Hanscomb, J. of Appl. Phys. 41, 3597 (1970).
14. Prof. Y.R. Shen has suggested (private communication) that local field effects may be important in an electron avalanche and may explain the difference in absolute field strenghts between d.c. and optical frequencies. The damage fields reported in the literature, however, are not corrected for local fields because it is normally assumed that any local field effects are averaged out by the electrons' rapid movement across the unit cell. The validity of this latter assumption has not been established.

TABLE I
EXPERIMENTAL BREAKDOWN FIELDS AND
CALCULATED SELF-FOCUSING PARAMETERS IN NaCl

PULSEWIDTH (10^{-12} sec)	P_{input} (10^6 watts)	P_c (10^6 watts)* electrostriction	electronic	E_{rms} (10^6 volts/cm) relative	absolute
15	1.5	2.9×10^4	18	$E(15\text{ps})/E(300\text{ps})$	12.4 ± 3.7
300	0.22	82	18	$= 2.6 \pm 0.7$	4.7
4.7×10^3 [†]	0.030	1.8	18	$E(4.7\text{ns})/E(10.3\text{ns})$	2.3 ± 0.4
10.3×10^3 [†]	0.033	1.8	18	$= 1.1 \pm 0.05$	2.1

* P_c is the calculated critical power for catastrophic self-focusing. The calculation of the electrostrictive value is discussed in Ref. 4. The electronic value is estimated from measurements of third harmonic generation as noted in Ref. 6.

[†]Results taken from Ref. 4.

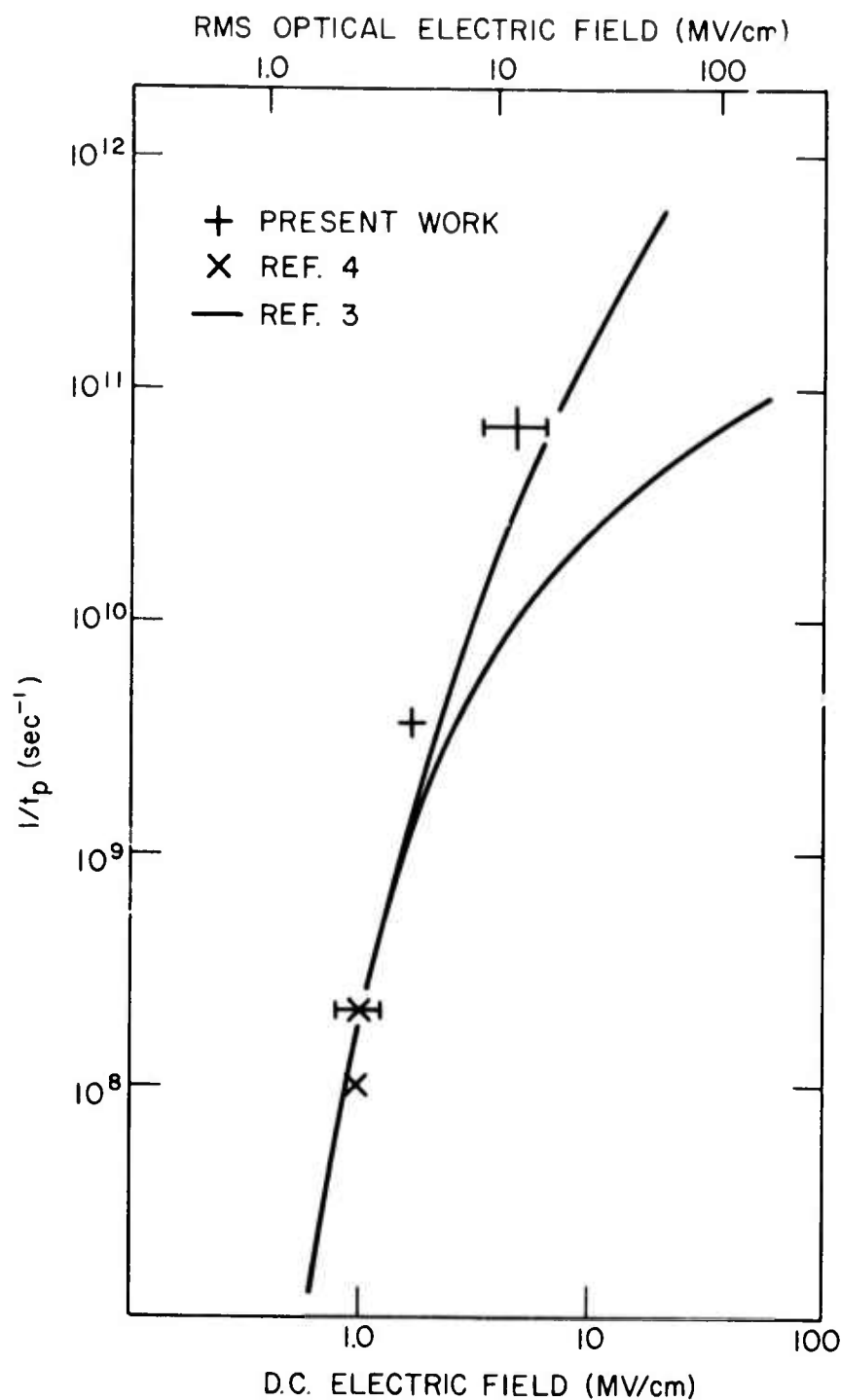


Fig. 1 - The functional relationship between the optical breakdown field strength and the pulse duration. The experimental points are compared with two semi-empirical drawn curves. (A discussion of these curves is given in the text and in Ref. 3.) The experimental error bars reflect experimental uncertainties in the absolute field strengths.

APPENDIX D



ILC Technology

ILC Report
R-ILC-73-8

10 April 1973

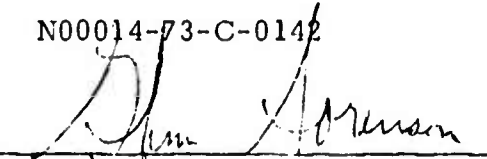
DISC LASER AMPLIFIER

by: Jack Moffat, Jr.

Prepared for: Naval Research Laboratory
4555 Overlook Avenue, S.W.
Washington, D.C.

Contract No: N00014-73-C-0142

APPROVED:


G. Sorenson, President

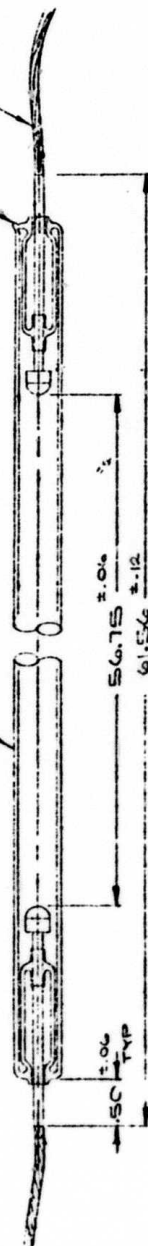
"Work Supported by Advanced Research Project Agency under ARPA Order 2062."

164 Commercial Street □ Sunnyvale, California 94086 □ Phone 408/738-2944

REVISIONS		
LTR	DESCRIPTION	DATE
A	REV/ECN 121	3/1/70
B	REV/ECN 159	8/1/70

13.9 MM OD NOM

TIP OFF 1
KULGRID 6 LG MIN TYP



1. TIP OFF HEIGHT 0.00 MAX
2. ENVELOPE MAT'L: 2MM WALL
CLEAR FUSED QUARTZ
3. MAX NON-FLEXIBLE LENGTH 62.3"

ITEM NO.	QTY	RECD	CODE IDENT	PART OR IDENTIFYING NO.	NOMENCLATURE OR DESCRIPTION
UNLESS OTHERWISE SPEC. TO BE ILC INC.			154 COMMERCIAL STREET SUNNYVALE, CALIFORNIA 94086		
TITLE			LAMP XENON FLASH		
DRAWN			DATE		
CHECK			APPROVED		
MATERIAL:			SIZE		
FINISH:			CODE IDENT. NO.		
NEXT ASSY			B 31573		
USED ON			DWG. NO.		
APPLICATION			11970		
			SCALE		
			SHEET		
			OF		